RSC Advances

Synthesis, structural properties, electrophilic substitution reactions and DFT computational studies of calix[3]benzofurans

Journal:	*RSC Advances*
Manuscript ID	RA-ART-03-2016-006219.R1
Article Type:	Paper
Date Submitted by the Author:	n/a

Complete List of Authors:	Islam, Md. Monarul; Saga University, Department of Applied Chemistry, Faculty of Science and Engineering; Bangladesh Council of Scientific and Industrial Research(BCSIR), Chemical Research Division Akther, Thamina; Saga University, Department of Applied Chemistry, Faculty of Science and Engineering Ikejiri, Yusuke; Saga University, Department of Applied Chemistry, Faculty of Science and Engineering Matsumoto, Taisuke; Kyushu University, Institute for Materials Chemistry and Engineering Tanaka, Junji; Kyushu University, Institute for Materials Chemistry and Engineering Rahman, Shofiur; Memorial University of Newfoundland, Chemistry; Saga University, Applied Chemistry Georghiou, Paris; Memorial University of Newfoundland, St. John's, Newfoundland and Labrador, Department of Chemistry Hughes, David; University of East Anglia Redshaw, Carl; University of Hull, Department of Chemistry Yamato, Takehiko; Faculty of Science and Engineering, Department of Chemistry and Applied Chemistry

Subject area & keyword:	Supramolecular - Organic < Organic

Synthesis, structural properties, electrophilic substitution reactions and DFT computational studies of calix[3]benzofurans

Md. Monarul Islam,[a,b] Thamina Akther, [a] Yusuke Ikejiri,[a] Taisuke Matsumoto,[c] Junji Tanaka,[c] Shofiur Rahman,[d] Paris E. Georghiou,[d] David L. Hughes,[e] Carl Redshaw[f] and Takehiko Yamato*[a]

Calix[3]benzofurans have been synthesized by a modified TosMIC coupling reaction, followed by acid treatment and an intramolecular cyclization reaction with TMSI (trimethylsilyl iodide); X-ray analysis established the structures of two samples, both showing a *cone* conformation. ^{1}H NMR spectroscopic analyses of the calix[3]benzofurans reveal that they can adopt drastically different conformations in solution and undergo very fast conformational changes relative to the NMR time scale. Calix[3]benzofuran **4a** exists as two conformers, namely the *cone* and *saddle* forms, in a ratio of 83:17 at -50 °C. A series of calix[3]benzofuran derivatives was synthesized by electrophilic aromatic substitutions, such as bromination, formylation and acylation, to investigate the influence of the substituents on the conformations of the calix[3]benzofurans. ^{1}H NMR spectral analyses of the acyl derivatives at room temperature indicated that these macrocycles exist as a mixture of two isomers that are slowly interconverted on the ^{1}H NMR timescale. The conformational isomers of the calix[3]benzofurans and their derivatives obtained from DFT methods (based on the crystal structure analysis results) were used to estimate the total energies of the different conformations.

Introduction

The design and synthesis of medium and larger sized ring systems is an area of current interest in supramolecular chemistry.[1] In particular, macrocycles containing aromatic groups represent a vital class of synthetic receptors in molecular recognition due to the hydrophobicity and π-stacking interactions of their aromatic groups.[2] Calixarenes and their analogues are receiving considerable attention because of their design possibilities as host molecules in supramolecular chemistry.[3] One of the characteristic properties of calixarenes is conformational variety.[4] By using this variety and design possibilities, calixarenes and their analogues can be useful as basic skeletons for molecular device units in molecular nanotechnology.[5]

Calix[3]benzofurans are calixarene derivatives in which the benzene rings have been replaced by benzofuran rings. Among the arenofurans, benzofurans are very interesting *O*–heterocycles and numerous synthetic methods have been developed for their preparation.[7–10] A major route for the synthesis of various arene ring-fused furan derivatives is the intramolecular formation of a furan moiety starting from properly substituted arene compounds *via* dehydrative cyclization of a carbonyl group.[6–11] The Prins cyclization reaction which generally involves a reaction between an aldehyde and a homoallylic alcohol promoted by acid is important for the construction of oxygen-containing heterocyclic units.[12] Many reactions have utilized upper/lower rim modification for the synthesis of new functionalized calixarenes.[13] Biali and co-workers have synthesized an interesting series of molecules, namely "bis(spirodienones)" prepared by the intramolecular oxidative cyclization through the phenolic hydroxyls of calix[4]arene.[14] Black and co-workers reported for the first time that some activated benzofuranylmethanols undergo acid-catalyzed cyclo-oligomerisation *via* electrophilic reactions to afford a range of calix[3]benzofurans and calix[4]benzofurans having π-electron rich cavities.[15] Although there have been extensive studies of calix[4]arenes over the last few decades,[16] reports on the preparation and characterization of calix[3]arenes have been very limited.[15] However, the synthetic potential of these molecules for the design of new macrostructures based on their structural features *viz*. calixarene analogues of metacyclophanes containing benzofuran rings linked by methylene bridges and DFT computational studies thereof, remains mostly unexplored. There are very few reports of DFT computational studies of calixarene analogues. Choe *et al* have reported DFT calculations on the conformational characteristics and hydrogen bonding of both *p-tert*-butylcalix[4]arene and *p-tert*-butylcalix[5]arene using the B3LYP/6-31+G(d,p) method.[17]

In our laboratory, we are now focusing on synthesizing calixarene-type metacyclophanes, with particular interest in their conformations and potential application.[18] The first objective of this research is to synthesize the calix[3]benzofurans and their derivatives by electrophilic substitution reactions such as bromination, formylation and acylation with a view to investigating their conformational properties. The second objective is to determine the energy of different conformational isomers of the calix[3]-benzofurans and derivatives using DFT computational studies.

Results and Discussion

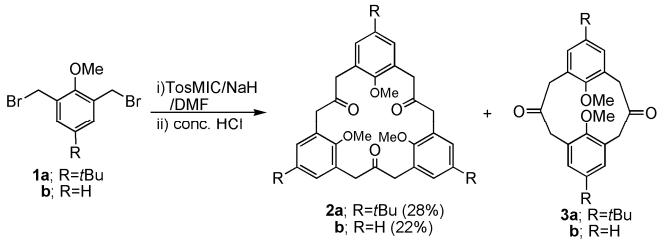

Scheme 1 Synthesis of 9,18,27-trimethoxy[3.3.3]MCP-2,11,20-triones **2**.

The synthetic routes and yields of [3.3.3]MCP-2,11,20-triones **2a–b** are shown in Scheme 1. The direct coupling reaction of (*p*-tolylsulfonyl)methyl isocyanide (TosMIC) with **1a–b** in the presence of NaH, followed by acid treatment, afforded the tri-ketones **2a–b** along with the dimers *anti/syn*-[3.3]MCP-2,11-diones **3a–b**, respectively.[19] In general, a mixture of TosMIC and **1a–b** in *N,N*-dimethylformamide (DMF) was added dropwise to a suspension of NaH in DMF at room temperature. 6,15,24-Tri-*tert*-butyl-9,18,27-trimethoxy[3.3.3]MCP-2,11,20-trione **2a** has been reported previously (Scheme 1).[19c] The structure of 9,18,27-trimethoxy [3.3.3]MCP-2,11,20-trione **2b** was elucidated by elemental analysis and spectral data. For instance, the mass spectral data for **2b** (M^+ = 486.23) strongly supported a cyclic trimeric structure. The IR spectrum of **2b** shows the absorption of the carbonyl stretching vibration at around 1716 cm^{-1}. The ^1H NMR spectrum of macrocycle **2b** exhibits two single peaks at δ 3.28 and 3.63 ppm for the methoxy protons and the ArCH_2COCH_2Ar methylene protons.

The cyclization of ketones **2a–b** with phenolic hydroxyl groups produced by treatment with TMSI (generated *in situ* from TMSCl and NaI in CH_3CN) led to the formation of the furan moiety instead of the expected product **4′** (Scheme 2). Thus nucleophilic intramolecular cyclization of intermediate **4′** afforded the calix[3]-benzofurans, **4a** and **5a** (Scheme 3). Sawada and co-workers have reported hemisphere-shaped calixarene analogues *via* a single step reaction involving a pinacol rearrangement followed by an intramolecular acetalization from tetrahydroxy-tetramethoxy-[2.1.2.1]MCP.[20] ^1H NMR spectroscopy demonstrates that calix[3]-benzofurans **4a** and **5a** adopt radically different conformations in solution at room temperature and undergo very fast conformational changes relative to the NMR time scale. To establish the conformation of **4a**, we carried out variable temperature (VT) NMR spectroscopy over the range -50 °C to +70 °C (Fig. 1).

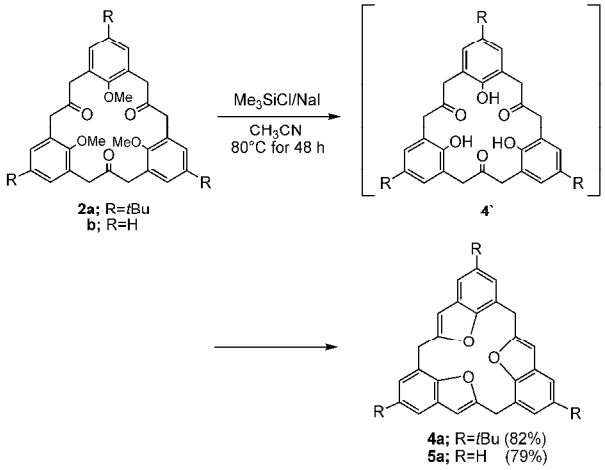

Scheme 2 Synthesis of calix[3]benzofurans **4a** and **5a**.

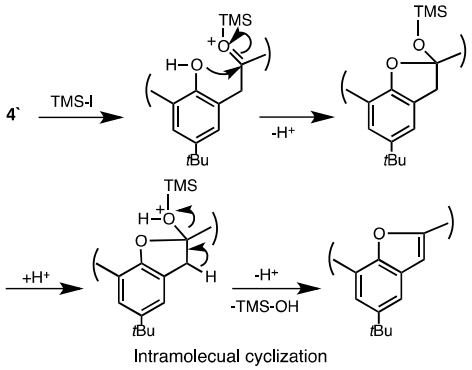

Scheme 3 Mechanism for formation of furan moiety.

The ^1H NMR spectrum at -50 °C suggests that the two conformers *cone* and *saddle* of calix[3]benzofuran **4a** exist in a ratio of 83:17. The interconversion of the conformational structures in solution are readily studied by variable-temperature ^1H NMR spectroscopic techniques by simply monitoring the change in the signals of the bridging methylene protons.[2b] The *cone* conformation was assigned by the observation of a set of doublets for the methylene protons at δ 4.1 and 4.7 ppm, whereas for the *saddle*, the methylene protons appear as a singlet at δ 4.2 at -50 °C (Fig. 1). The bridging methylene protons are in different chemical environments (*axial* and *equatorial*), but quickly interconvert on the NMR time scale at room temperature and appear as a singlet or broad peak.

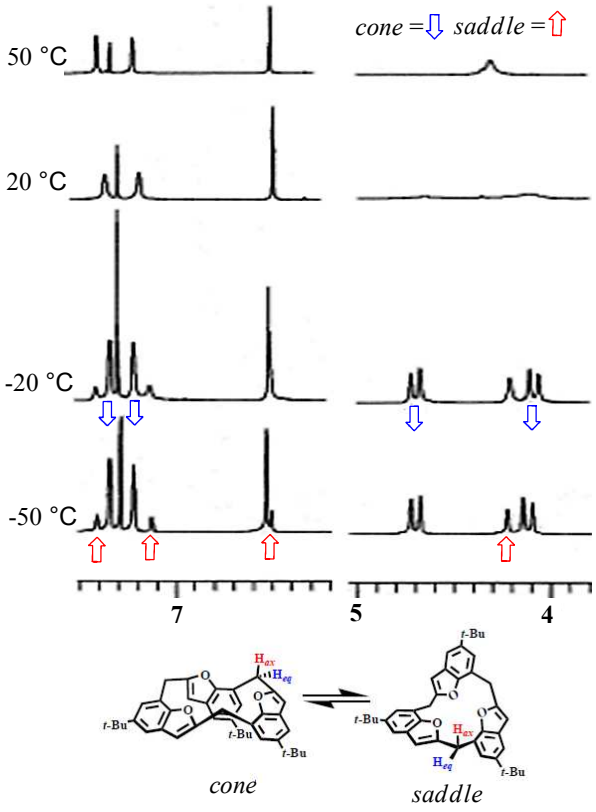

Fig. 1 Partial VT-NMR spectra of 6,14,22-tri-*tert*-butylcalix[3]-benzofuran **4a** in $CDCl_3$.

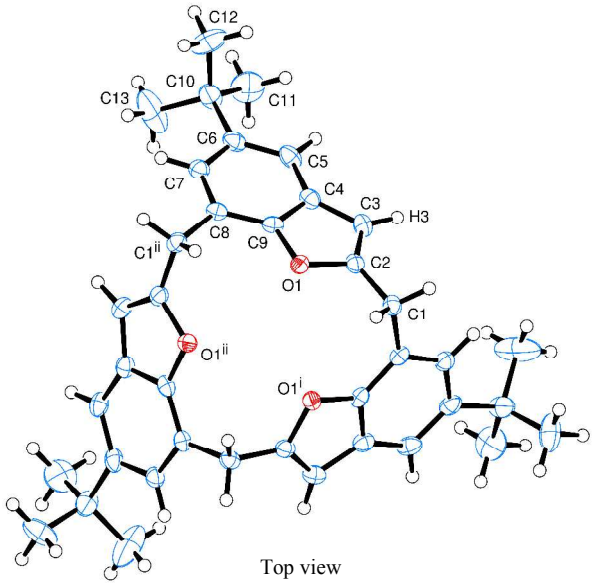

Fig. 2 Ortep drawing of **4a**. Thermal ellipsoids are drawn at the 50 % probability level. All hydrogen atoms are omitted for clarity.

When the temperature is dropped sufficiently, the conformation becomes more rigid and the interconversion is slower than NMR time scale, which causes the CH_2 signal to resolve into a pair of doublets. Single crystals of **4a** (CCDC-1456536) were grown from a hexane solution, and were investigated by X-ray crystallography to confirm the conformation; the crystal structure was found to belong to the trigonal crystal system with space group R-3 (SI Table S1). Although calix[3]benzofuran **4a** forms drastically different conformations in solution at room temperature, it adopts a rigid *cone* type hemisphere shaped symmetrical structure in the solid state (Fig. 2).

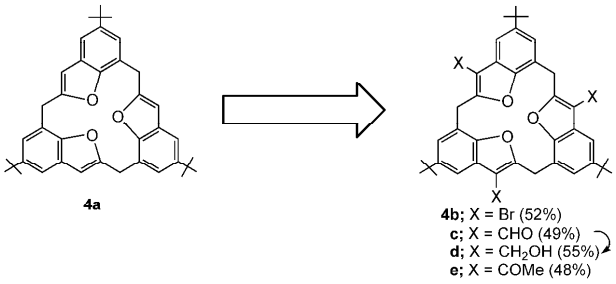

Scheme 4 *Reagents and conditions:* (a) BTMA Br_3, CH_2Cl_2, r.t. 24 h, 52 %; (b) Cl_2CHOCH_3, $TiCl_4$, CH_2Cl_2, r.t. 3 h, 49 %; (c) $NaBH_4$, $EtOH/CH_2Cl_2$, reflux 24 h, 55 %; (d) AcCl, $TiCl_4$, CH_2Cl_2, r.t. 3 h, 48 %.

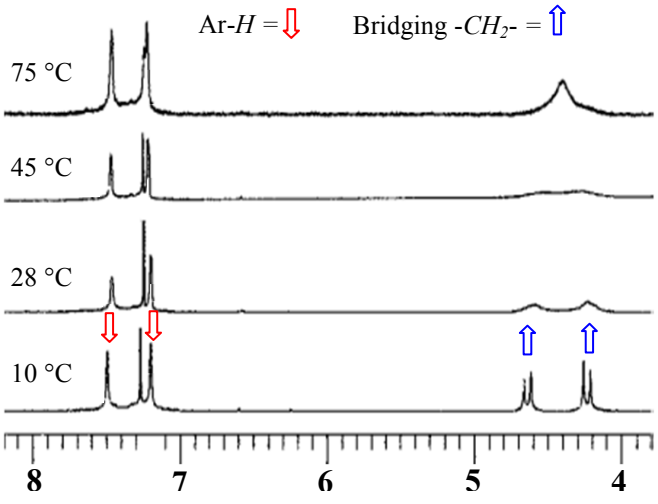

Fig. 3 Partial VT-NMR of 4,12,20-tribromo-6,14,22-tri-*tert*-butyl-calix[3]benzofuran **4b** in $CDCl_3$ (300 MHz).

Thus, it freely interconverts between the *cone* and *saddle* conformations in solution. Since the conformation of calix[3]benzofuran is not clear at room temperature in solution where both the *cone* and *saddle* conformation exist, to investigate further the detailed conformational structure, a series of electrophilic substitution reactions was carried out, such as bromination, formylation and acetylation, at the furan moieties (Scheme 4).

To investigate the substituent effects on the conformation, we commenced our study by bromination of 6,14,22-tri-*tert*-butylcalix-[3]benzofuran **4a** with benzyltrimethylammonium tribromide (BTMA-Br_3) in CH_2Cl_2 at room temperature, which afforded only the rigid *cone*-4,12,20-tri-bromo-6,14,22-tri-*tert*-butylcalix[3]benzo-furan **4b**. Two broad single peaks at δ 4.24 and 4.60 ppm in the ^{1}H NMR ($CDCl_3$, 400 MHz) spectrum were evidence for the formation of the fixed *cone* type conformer in solution at room temperature (SI, Fig. S9). However at 10 °C, the two broad peaks split into two clearly defined doublets established the formation of the *cone* conformation (Fig. 3). The structure of the macrocycle **4b** was confirmed by single-crystal X-ray analysis (CCDC-1456535) and an ORTEP drawing is shown in Fig. 4. The analysis shows the well-defined calixarene molecule lying around a threefold symmetry axis with, on one side, a $CHCl_3$ solvent molecule (also on the symmetry axis and well-defined) and, on the other side, a complex ring structure, presumably of a disordered array of methanol molecules; in this region, 50 atoms have been refined as isotropic carbon atoms mostly with site occupancies of 0.5, about a point of *-3* symmetry.

Formylation of 6,14,22-tri-*tert*-butylcalix[3]benzofuran **4a** with 1,1-dichlorodimethyl ether in the presence of $TiCl_4$ at room temperature afforded 6,14,22-tri-*tert*-butyl-4,12,20-triformylcalix[3]-benzofuran **4c**. On replacement of bromine by a more electron withdrawing group (-CHO) at the furan moiety, it is seen that the conformation of **4c** in solution at room temperature underwent very fast changes relative to the ^{1}H NMR timescale and gave a broad peak for bridging methylene protons at δ 4.59 ppm (SI, Fig. S11), consistent with an equilibrium existing between the *cone* and the *saddle* conformations. However at low temperature (-30 °C), the isomerization between *cone* and *saddle* is slow and the *saddle* is the major conformation in solution (Table 1). Thus, different conformational properties of 6,14,22-tri-*tert*-butylcalix[3]benzofuran **4a** were observed upon changing the group at the furan moiety. We then introduced the medium-sized CH_2OH group by reduction of

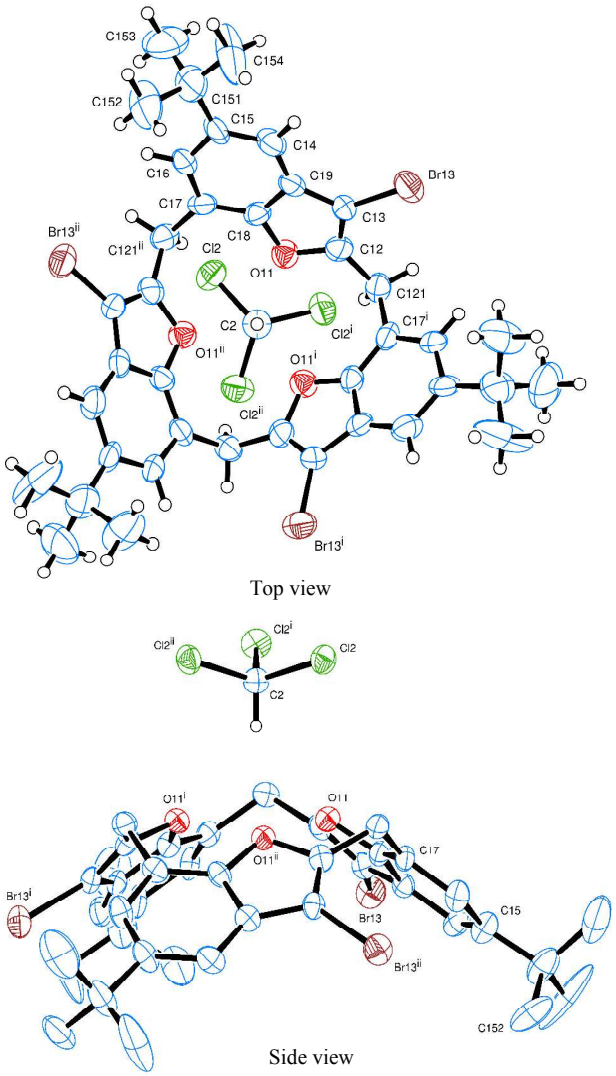

Fig. 4 Ortep drawing of **4b**. Thermal ellipsoids in the top view are drawn at the 50 % probability level and those in the side view at 30 %. In both views, the cluster of disordered solvent methanol molecules has been omitted.

4c with $NaBH_4$, which afforded 6,14,22-tri-*tert*-butyl-4,12,20-trihydroxymethylcalix[3]benzofuran **4d**. The CH_2OH group has no significant electron withdrawing power and it is surprising that the conformation of the 6,14,22-tri-*tert*-butyl-4,12,20-trihydroxymethylcalix[3]benzofuran **4d** dramatically converted to a fixed *cone* conformation as in compound **4b**. The bridging methylene groups appear as broad singlets and gives peaks at δ 4.22 and 4.66 ppm (SI, Fig. S13).

Table 1. Influence of substituents on the conformation of benzofurans.

Compound	T_c (°C)	$\Delta G^{\ddagger}$ (kJ mol^{-1})	*cone:saddle* (-30 °C)
4a; X = H	40[a]	61.9 (J = 14.8 Hz)	80:20
4b; X = Br	45[a]	62.8 (J = 14.4 Hz)	100:0
4c; X = CHO	28[a]	58.6 (J = 13.5 Hz)	40:60
4d; X = CH_2OH	50[a]	68.2 (J = 14.4 Hz)	100:0
4e; X = COMe	75[b]	69.0 (J = 13.2 Hz)	20:80

[a] Solvent: $CDCl_3$; [b] Solvent: $CDBr_3$. (300 MHz)

Bromine is electron withdrawing in nature, but the multiple lone-pairs of electrons are able to increase electron density at the furan moiety and fix the conformation of **4b** to the *cone* conformation. Although the -CH_2OH group has less electron withdrawing power than the formyl group (-CHO), the alcohol group (-CH_2OH) is slightly larger, and so steric effects come into play and the molecule is generally locked in one conformation *i.e.* stabilization of the ring occurs. Thus, both the electron withdrawing ability and the steric hindrance play a significant role on the conformational preferences of calix[3]benzofuran derivatives. With these results in hand, we elaborated our study by introducing the larger acyl-group (-COMe), which has less electron withdrawing ability than CHO, but is larger than CH_2OH, in order to investigate the effects on the conformation of the calix[3]benzofuran derivatives. Treatment of 6,14,22-tri-*tert*-butylcalix[3]benzofuran **4a** with acetyl chloride in the presence of $TiCl_4$ at room temperature afforded 4,12,20-triacetyl-6,14,22-tri-*tert*-butylcalix[3]benzofuran **4e**.

^{1}H NMR spectral analyses of the acylation derivatives indicate that these macrocycles exist as a mixture of two conformers that slowly interconvert on the ^{1}H NMR timescale. This is evident from the two distinct ^{1}H signals observed for the bridging methylene protons that appear as two sets of doublets at δ 4.62 and 4.49 ppm for the *cone* conformation and a single peak at δ 4.55 ppm for the *saddle* conformation (SI, Fig. S15). In this case, the acyl group (-COMe) makes the furan ring electron deficient as in the case of the formyl group (-CHO), but due to the larger size of the acyl group (-COMe), it is possible that steric hindrance prevents complete rapid isomerization at room temperature in solution. At -30 °C, the isomerization between *cone* and *saddle* is very slow and the major conformation is *saddle* (Table 1); a similar result was observed for the electron withdrawing formyl derivative of calixbenzofuran **4c**. So, both electronic and steric effects of the substituents can play a significant role on the conformation of calix[3]benzofuran derivatives and can lead to interesting conformational changes in solution. In view of the encouraging results in conformational changes obtained by electrophilic substitution reactions of **4a**, we extended our studies towards the calix[3]benzofuran **5a**.

Similar types of phenomena were observed when calix[3]-benzofuran **5a** was reacted with acetyl chloride at room temperature in the presence of $TiCl_4$; the product was 4,12,20-triacetylcalix[3]-benzofuran **5b** (Scheme 5). ^{1}H NMR (SI, Fig. S17) spectroscopic analysis of **5b** indicates that this macrocycle also exists as a mixture of two conformers that are slow to interconvert on the ^{1}H NMR timescale at room temperature. This is evident by two distinct signals observed for the bridging methylene protons that appear as two doublets at δ 4.68 and 4.99 ppm for the *cone* conformer and a single peak at δ 4.58 ppm for the *saddle* conformation (SI, Fig. S17). Acylation of macrocycle **5a** indicates that the furan ring in benzofuran is electron rich and electrophilic substitution occurs preferentially in this ring rather than the benzene ring and that the *tert*-butyl groups have no significant effect on the conformation of calix[3]benzofuran.

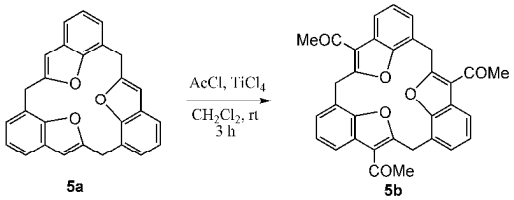

Scheme 5 Acetylation of calix[3]benzofuran **5a**.

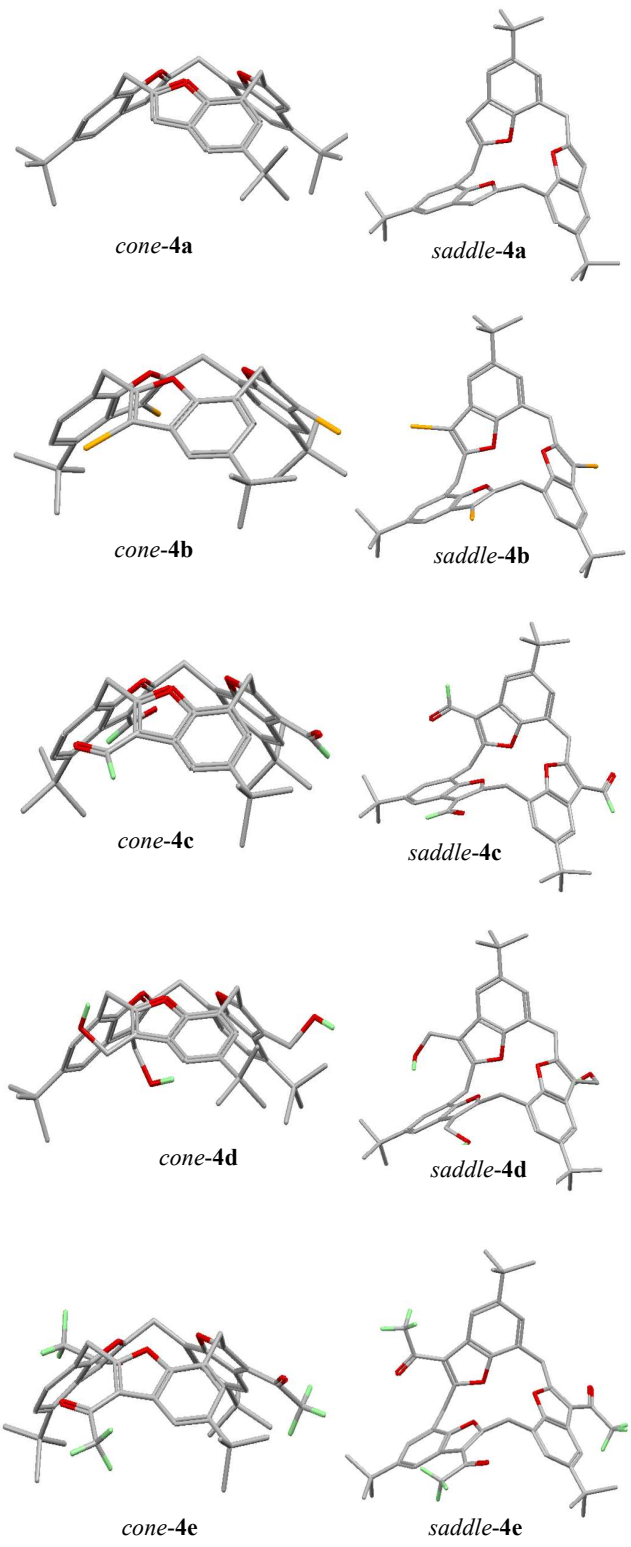

Fig. 5 DFT B3LYP/6-31G(d) optimized molecular structures of the *cone* (left) and *saddle* (right) of (i) **4a**, (ii) **4b**, (iii) **4c**, (iv) **4d** and (v) **4e** in $CHCl_3$ solvent.

It is important to emphasize that all the synthesized calix[3]-benzofuran derivatives gave only two sets of distinct proton

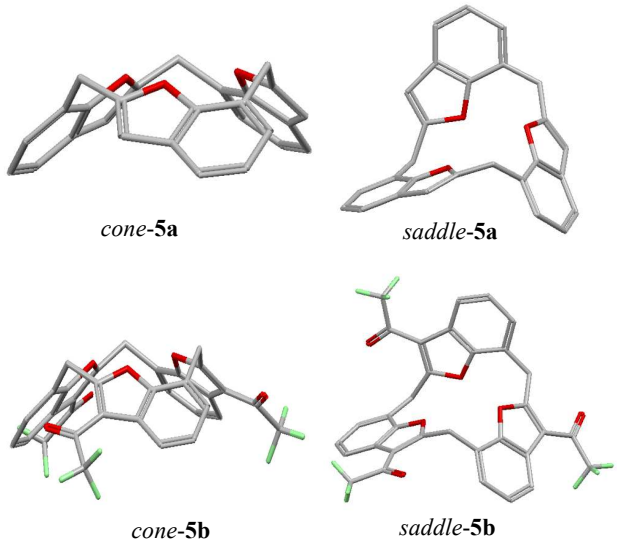

Fig. 6 DFT B3LYP/6-31G(d) optimized molecular structures of the *cone* (left) and *saddle* (right) of (i) **5a** and (ii) **5b** in $CHCl_3$ solvent.

resonances in their ^{1}H NMR spectra for the methylene bridge. The ^{1}H NMR spectra indicated clearly that **4d** adopts a shape-persistent *cone* conformation, whereas **4c** derivatives exist as equilibrium mixtures in which various conformers (*cone* and *saddle*) undergo rapid interconversion relative to the ^{1}H NMR time scale evident by a broad peak at δ 4.59 ppm. However, **4e** underwent very slow interconversion relative to the ^{1}H NMR time scale giving two sets of doublets at δ 4.62 and 4.49 ppm for the *cone* conformation and a single peak at δ 4.55 ppm for the *saddle* conformation.

The conformations of the present system have also been evaluated by means of dynamic ^{1}H NMR spectroscopy. By observation of the resonances arising from the ArCH_2Ar methylene protons, the coalescence temperatures (T_c) and free energy barriers ($\Delta G^{\ddagger}$) have been estimated (Table 1). This behavior indicates that the rate of conformational ring flipping of these macrocycles is faster than the NMR time scale above this temperature (T_c). Density functional theory (DFT) computational studies were carried out to determine the geometry-optimized energies of all the synthesized calix[3]benzofurans **4a**–**e** and **5a**–**b** (SI Table S2 and Table S3). The starting structures were generated with initial geometries based upon the X-ray structures of **4a** and 4**b** and from the presumed structures of **4c**–**4d** (derived from *cone*-**4a** and *cone*-4**b**) and **5a**–**b** using *SpartanPro'10* with the MMFF94 method.[22] The individual geometry-optimized structures of these molecules in both $CHCl_3$ solvent (Fig. 5 and Fig. 6) and in the gas phase were optimized using Gaussian 09 with the B3LYP level of theory and the 6-31G(d) basis set.[23] The computed energies of the two distinct conformers and their energy differences (ΔE, kJ mol^{-1}), are listed in Tables 2 and 3 (and SI Tables S2 and S3). From the DFT-optimized B3LYP/6-31G(d) computed energies of all of the synthesized calix[3]benzofurans **4a**–**e** and **5a**–**b**, it is seen that both the *cone* and *saddle*-conformations have lower ground-state energies in the solvent system than in the gas phase (Table 3). Furthermore, the DFT optimized B3LYP/6-31G(d) energies of *tert*-butylcalix[3]- benzofurans **4a** and derivatives **4b**–**e**, suggest that the *saddle* conformer is energetically more stable than the *cone* isomer (Table 3). Although **4a** and **4b** adopt *cone* conformations in the solid state (Fig. 2 & 3), the DFT optimized B3LYP/6-31G(d) energies of these two conformers imply that the *saddle* conformers of **4a** and **4b** are –4 and –35 kJ mol^{-1}, more stable

than the *cone* conformers in the solvent, with similar results in the gas phase (Table 3). On the other hand, in calix[3]benzofuran **5a** and its derivative **5b** (without *tert*-butyl groups), the *saddle* conformers are energetically less stable than the *cone* conformers by 4 and 10 kJ mol^{-1} in the gas phase, and by 5 and 7 kJ mol^{-1} in solvent (Table 3), respectively. Similarly, *saddle*-**4c**, **4d**, **4e** are energetically more stable by 12, 20 and 48 kJ mol^{-1} than *cone*-**4c**, **4d**, **4e** in the gas phase, respectively (Table 3).

Table 2. Geometry optimization energies using B3LYP/6-31G(d) ($\Delta E = E_{chlorofom} - E_{gas\text{-}phase}$)

	cone	***saddle***
Compound	ΔE kJ mol^{-1}	ΔE kJ mol^{-1}
4a	-17	-17
5a	-18	-17
4b	-13	-15
4c	-23	-28
4d	-35	-31
4e	-26	-28
5b	-25	-28

The results presented in Table S2 and Table S3 show that among the calix[3]benzofurans, **4b** is the energetically most-favored (in both the solvent and gas-phase) and the order is as follows: **4b** > **4e** > **4d** > **4c** > **4a** > **5b** > **5a** in both the solvent and gas phase.

So by introducing the different groups at the furan moieties, the derivatives become energetically more favored over the corresponding calix[3]benzofuran according to the increasing size of groups (i.e. COMe > CH_2OH > CHO) except for **4b**. In the case of **4b**, there may be two factors influencing the stability: bromine is electronegative in nature and it has greater electron-density due to multiple lone-pairs of electrons.

Table 3. Geometry optimization energies using B3LYP/6-31G(d) ($\Delta E = E_{Saddle} - E_{Cone}$)

	Gas-phase	**Chloroform**
Compound	ΔE kJ mol^{-1}	ΔE kJ mol^{-1}
4a	-4	-4
5a	4	5
4b	-34	-35
4c	-12	-18
4d	-20	-16
4e	-48	-50
5b	10	7

Conclusions

We have described a simple and effective method for the synthesis of flexible calix[3]benzofurans by introducing furan moieties through intramolecular cyclization of [3.3.3]MCP-trione. To explore the rates of conformational interconversion of the described calix[3]benzofurans, a series of electrophilic substitution reactions such as bromination, formylation and acylation reactions of calix[3]benzofurans were studied. The presence of bromine or an alcohol group (-CH_2OH) at the furan ring led to the adoption of the fixed *cone* conformation, whereas the presence of the larger -COMe forced the adoption of both the *cone* and *saddle* conformations in solution and very slow interconvertion on the ^{1}H NMR timescale at room temperature. However, the formyl derivative exhibits rapid conformational transformation as for the calix[3]benzofurans. Conformational flexibility of calix[3]benzofuran derivatives was observed by controlling the steric crowding and electron withdrawing ability of the groups. The DFT computational optimized B3LYP/6-31G(d) molecular energies of all synthesized tri-*tert*-butylcalix[3]benzofurans were determined, and revealed that the *saddle* conformers were energetically favoured over the corresponding *cone* conformers; in the calix[3]benzofurans without *tert*-butyl groups, the *cone* conformers were the more stable. Further mechanistic details of calix[3]benzofuran derivatives are being explored (by introducing different groups and resolution of their isomers), and will be reported in due course.

Acknowledgments

We would like to thank the OTEC at Saga University for financial support. This work was performed under the Cooperative Research Program of "Network Joint Research Center for Materials and Devices (Institute for Materials Chemistry and Engineering, Kyushu University)". CR thanks the EPSRC for a travel award.

Experimental

General

All melting points (Yanagimoto MP-S1) are uncorrected. Proton nuclear magnetic resonance (^{1}H NMR) spectra and ^{13}C NMR spectra were recorded on Nippon Denshi JEOL FT-300 NMR and Varian-400MR-vnmrs400 spectrometers. Chemical shifts are reported as δ values (ppm) relative to internal Me_4Si. Mass spectra were obtained on a Nippon Denshi JMS–01SA–2 mass spectrometer at ionization energy of 70 eV; *m/z* values reported include the parent ion peak. Infrared (IR) spectra were obtained on a Nippon Denshi JIR-AQ2OM spectrophotometer as KBr disks. Elemental analyses were performed by Yanaco MT-5. G.L.C. analyses were performed by Shimadzu gas chromatograph, GC-14A; Silicone OV–1, 2 m; programmed temperature rise, 12 °C min^{-1}; carrier gas nitrogen, 25 mL min^{-1}. Silica gel columns were prepared by use of Merk silica gel 60 (63–200 μm)

Materials

The preparation of 2,6-bis(bromomethyl)-4-*tert*-butylanisole **1a** and 2,6-bis(bromomethyl)anisole **1b** were previously described.[21] 6,15,24-Tri-*tert*-butyl-9,18,27-trimethoxy[3.3.3]MCP-2,11,20-trione **2a** was prepared according to reported methods.[19c]

Direct cyclization of dibromide 1 with TosMIC

To a suspension of NaH (2.1 g, 51 mmol) in DMF (150 mL) a solution of **1a** (6.0 g, 17.1 mmol) and TosMIC (3.3 g, 22.0 mmol) in DMF (35.0 mL) was added dropwise over a period of 6 h. After the reaction mixture was stirred for an additional 5 h at room temperature, it was quenched with ice-water (300 mL). The reaction mixture was extracted with CH_2Cl_2 (100 mL × 3), washed with water (100 mL), dried over Na_2SO_4, and concentrated *in vacuo* to 15 mL. Concentrated HCl (15 mL) was added to the solution and stirring was continued for 15 min. The organic layer was again extracted with CH_2Cl_2 (100 mL × 3), washed with water (100 mL × 2), dried over Na_2SO_4, and concentrated and condensed under reduced pressure. The residue was chromatographed on silica gel using $CHCl_3$ as eluents to give crude **2a** as a pale yellow solid. Recrystallization from hexane afforded 6,15,24-tri-*tert*-butyl-9,18,27-trimethoxy[3.3.3]MCP-2,11,20-trione **2a** (912 mg, 28 %) as pale yellow prisms. M.p. 227–228 °C (lit.[20c] 217–218 °C). IR: ν_{max} (KBr)/cm^{-1}: 1720 (C=O). ^{1}H NMR (400 MHz, $CDCl_3$): δ = 1.19 (27H, s, *t*Bu × 3), 3.33

(9H, s, O*Me*), 3.61 (12H, s, CH_2) and 6.92 (6H, s, Ar–*H*) ppm. ^{13}C NMR (100 MHz, $CDCl_3$): δ = 31.41, 34.19, 44.10, 60.20, 126.87, 127.01, 146.51, 154.55 and 206.96 ppm. FABMS: *m/z*: 654.82 [M^+]. $C_{42}H_{54}O_6$ (654.90): calcd C 77.03, H 8.31; found: C 76.97, H 8.19.

Compound **2b** was similarly prepared.

9,18,27-Trimethoxy[3.3.3]MCP-2,11,20-trione 2b: Recrystallization from hexane afforded 9,18,27-trimethoxy[3.3.3]MCP-2,11,20-trione **2b** (640 mg, 22 %) as pale yellow prisms. M.p. 203–204 °C. IR: ν_{max} (KBr)/cm^{-1}: 1716 (C=O). ^{1}H NMR (400 MHz, $CDCl_3$): δ = 3.28 (9H, s, O*Me*), 3.63 (12H, s, CH_2), 6.94 (3H, t, *J* =7.6, Ar–*H*) and 7.04 (6H, d, *J* =7.6, Ar–*H*) ppm. ^{13}C NMR (100 MHz, $CDCl_3$): δ = 43.29, 60.22, 124.04, 128.12, 130.17, 156.97 and 205.78 ppm. FABMS: *m/z*: 486.23 [M^+], 487.23 [M^++1], $C_{30}H_{30}O_6$ (486.20): calcd C 74.06, H 6.21; found: C 73.83, H 6.21.

Demethylation of 2a with TMSI

To a solution of **2a** (200 mg, 0.3 mmol) in CH_3CN (10.0 mL), NaI (900 mg, 6.0 mmol) was added. After adding trimethyl silyl chloride (0.8 mL, 6.0 mmol), the mixture was stirred at 80–85 °C for 48 h. The reaction mixture was quenched in 20 mL ice water and 10% aqueous sodium thiosulphate solution (40 mL) was added and stirring continued for 1h at room temperature. Then the mixture was stirred with 10 % HCl (20 mL) for 1h and extracted with CH_2Cl_2 (40 mL × 3). The combined mixture was washed by 10 % $NaHCO_3$ (20 mL) and water (20 mL × 2) and dried over Na_2SO_4, and then concentrated under reduced pressure. The residue was chromatographed on silica gel using hexane:$CHCl_3$ (5:1) as eluents to give crude **4a** as a colourless solid. Recrystallisation from hexane afforded 6,14,22-*tri*-*tert*-butylcalix[3]benzofuran **4a** (138 mg, 82 %) as colourless prisms. M.p. 190–191 °C. IR: υ_{max} (KBr)/cm^{-1}): 2960, 2862, 1586, 1480, 1302, 1198, 867. ^{1}H NMR (400 MHz, $CDCl_3$): δ = 1.32 (27H, s, *t*Bu × 3), 4.09 (6H, brs, CH_2), 6.43 (3H, s, Ar–*H*), 7.13 (3H, s, Ar–*H*) and 7.31 (3H, s, Ar–*H*) ppm. ^{13}C NMR (100 MHz, $CDCl_3$): δ = 30.79, 31.89, 34.59, 102.62, 115.31, 121.43, 129.05, 145.72 and 157.74 ppm. FABMS: *m/z*: 558.35 [M^+]. $C_{39}H_{42}O_3$ (558.31): calcd C 83.83, H 7.58; found: C 83.53, H 7.58.

Compound **5a** was similarly prepared.

Calix[3]benzofuran 5a: Recrystallisation from hexane afforded calix[3]benzofuran **5a** (92 mg, 79 %). M.p. 180–181 °C. IR: υ_{max} (KBr)/cm^{-1}): 2962, 1429, 1194 and 810. ^{1}H NMR (400 MHz, $CDCl_3$): δ = 4.15 (6H, s, CH_2), 6.48 (3H, s, Ar–*H*), 7.08 (3H, t, *J* = 6.8, Ar–*H*) and 7.32 (6H, d, *J*=6.4, Ar–*H*) ppm. ^{13}C NMR (100 MHz, $CDCl_3$): δ = 30.35, 110.02, 119.20, 123.59, 129.38, 144.19 and 152.75 ppm. HRMS: *m/z*: 390.1253 [M^+]. $C_{27}H_{18}O_3$ (390.1256): calcd C 83.06, H 4.65; found: C 82.78, H 4.72.

Bromination of 6,14,22-tri-*tert*-butylcalix[3]benzofuran 4a

To a solution of **4a** (100 mg, 0.18 mmol) in CH_2Cl_2 (7.0 mL), $BTMABr_3$ (278 mg, 0.71 mmol) was added and the mixture was stirred for 24 h at room temperature. Then the mixture was extracted with CH_2Cl_2 (50 mL × 3) and the combined mixture was washed by water (20 mL × 2) and dried over Na_2SO_4, and then concentrated under reduced pressure. The residue was chromatographed on silica gel using CH_2Cl_2 as eluents to give crude **4b** as a yellow powder. Recrystallisation from methanol afforded 4,12,20-tribromo-6,14,22-tri-*tert*-butylcalix[3]benzofuran **4b** (75 mg, 52 %) as yellow prisms. M.p. 190–191 °C. IR: υ_{max} (KBr)/cm^{-1}): 2962, 2851, 1522, 1478, 1361, 1196, 867. ^{1}H NMR (400 MHz, $CDCl_3$): δ = 1.34 (27H, s, *t*Bu × 3), 4.22 (3H, brs, CH_2), 4.58 (3H, brs, CH_2), 7.21 (3H, s, Ar–*H*) and 7.47 (3H, s, Ar–*H*) ppm. ^{13}C NMR (100 MHz, $CDCl_3$): δ = 28.52, 31.70, 34.69, 114.12, 119.46, 124.27, 128.04, 146.76 and 152.68 ppm. FABMS: *m/z*: 793.90 [M^+]. $C_{39}H_{39}Br_3O_3$ (792.04): calcd C 58.89, H 4.94; found: C 58.64, H 4.81.

Formylation of 6,14,22-tri-*tert*-butylcalix[3]benzofuran 4a

To a solution of **4a** (100 mg, 0.18 mmol) and Cl_2CHOCH_3 (0.96 mL, 1.08 mmol) in CH_2Cl_2 (2 mL) was added a solution of $TiCl_4$ (0.12 mL, 1.08 mmol) in CH_2Cl_2 (2 mL) at 0 °C. After stirring the reaction mixture at room temperature for 2 h, it was poured into ice water (20 mL) and then the mixture was extracted with CH_2Cl_2 (50 mL × 3) and the combined mixture was washed by water (20 × 2 mL) and dried over Na_2SO_4, and then concentrated under reduced pressure. The residue was chromatographed on silica gel (Wako C-300, 500 g) using CH_2Cl_2 as eluents to give crude **4c** as a yellow powder. Recrystallisation from methanol afforded 6,14,22-tri-*tert*-butyl-4,12,20-triformylcalix[3]- benzofuran **4c** (57 mg, 49 %) as a yellow powder. M.p. 260–261 °C. IR: υ_{max} (KBr)/cm^{-1}): 2962, 1678 (C=O), 1434. ^{1}H NMR (400 MHz, $CDCl_3$): δ = 1.35 (27H, s, *t*Bu × 3), 4.59 (6H, brs, CH_2), 7.48 (3H, s, Ar–*H*), 8.02 (3H, s, Ar–*H*) and 10.41 (3H, brs, *CHO*) ppm. ^{13}C NMR (100 MHz, $CDCl_3$): δ = 29.33, 31.77, 34.95, 117.37, 124.20, 153.20, 157.06, 159.94, 166.36 and 196.67 ppm. HRMS: *m/z*: 642.2994 [M^+]. $C_{42}H_{42}O_6$ (642.2981): calcd C 78.48, H 6.59; found: C 78.45, H 6.81.

Preparation of 6,14,22-tri-*tert*-butyl-4,12,20-trihydroxymethylcalix[3]-benzofuran 4d

To a solution of **4c** (50 mg, 0.08 mmol) in a mixture of CH_2Cl_2 (2.0 mL), EtOH (2mL), $NaBH_4$ (27 mg, 0.7 mmol) was added and the system was reflux for 24 h. Then the mixture was extracted with CH_2Cl_2 (50 mL ×3) and the combined mixture was washed by water (20 mL × 2) and dried over Na_2SO_4, and then concentrated under reduced pressure. The residue was chromatographed on silica gel (Wako C-300, 500 g) using CH_2Cl_2 as eluents to give crude **4d**. Recrystallisation from hexane afforded 6,14,22-tri-*tert*-butyl-4,12,20-trihydroxymethylcalix[3]benzofuran **4d** (28 mg, 55 %) as a yellow powder. M.p. > 280 °C. IR: ν_{max} (KBr)/cm^{-1}: 3420, 2956, 2871, 1480, 1363, 1001. ^{1}H NMR (400 MHz, $CDCl_3$): δ = 0.89 (3H, brs, CH_2OH), 1.33 (27H, s, *t*Bu), 4.22 (3H, brs, CH_2), 4.66 (3H, brs, CH_2), 4.86 (6H, s, CH_2OH), 7.26 (3H, s, Ar–*H*) and 7.39 (3H, s, Ar–*H*) ppm. ^{13}C NMR (100 MHz, $CDCl_3$): δ = 28.71, 31.85, 34.75, 55.38, 114.20, 121.92, 128.46, 146.59, 150.30 and 155.25 ppm. HRMS: *m/z*: 648.3472. $C_{42}H_{48}O_6$ (648.3451): calcd C 77.75 H 7.46; found: 77.52 H 7.28.

Preparation of 4,12,20-triacetyl-6,14,22-tri-*tert*-butylcalix[3]-benzofuran 4e

To a solution of **4a** (100 mg, 0.18 mmol) and AcCl (0.08 mL, 1.08 mmol) in CH_2Cl_2 (2 mL) was added a solution of $TiCl_4$ (0.12 mL, 1.08 mmol) in CH_2Cl_2 (1 mL) at 0 °C and stirring was continued for 1 h. Then the mixture was stirred at room temperature for 3 h and poured into ice water. Then the mixture was extracted with CH_2Cl_2 (50 mL × 3) and the combined mixture was washed by water (20 mL × 2) and dried over Na_2SO_4, concentrated under reduced pressure. The residue was chromatographed on silica gel (Wako C-300, 500 g) using CH_2Cl_2 as eluents to give crude **4e** as a yellow powder. Recrystallisation from hexane afforded 4,12,20-triacetyl-6,14,22-tri-*tert*-butylcalix[3]benzofuran **4e** (59 mg, 48 %) as a yellow powder. M.p 164–165 °C. IR: ν_{max} (KBr)/cm^{-1}: 2960, 2870, 1674, 1464, 1381, 1186. ^{1}H NMR (400 MHz, $CDCl_3$): δ = *con*e–1.38 (27H, s, *t*Bu × 3), 2.63 (9H, s, -COCH_3), 4.62 (3H, d, *J* = 13.2 Hz, CH_2), 4.93 (3H, d, *J* = 14.4 Hz, CH_2), 7.80 (3H, s, Ar–*H*), 7.88 (3H, s, Ar–*H*), *saddle*–1.36 (27H, s, *t*Bu × 3), 2.63 (9H, s, -COCH_3), 4.55 (6H, s, CH_2), 7.38 (3H, s, Ar–*H*) and 7.54 (3H, s, Ar–*H*) ppm. ^{13}C NMR (100 MHz, $CDCl_3$): δ = 29.32, 31.32, 31.83, 34.88, 116.49, 117.34, 119.04, 123.96, 125.70, 147.46, 163.25 and 194.24 ppm. HRMS: *m/z*: 684.3453 [M^+]. $C_{45}H_{48}O_6$ (684.3451): calcd C 78.92 H 7.06; found: C 78.83, H 7.28.

Preparation of 4,12,20-triacetylcalix[3]benzofuran 5b

To a solution of **5a** (70 mg, 0.18 mmol) and CH_3COCl (0.076 mL, 1.08 mmol) in CH_2Cl_2 (2 mL) was added a solution of $TiCl_4$ (0.12 mL, 1.08 mmol) in CH_2Cl_2 (2 mL) at 0 °C. After stirring the reaction mixture at room

temperature for 2 h, it was poured into ice water (20 mL) and then the mixture was extracted with CH_2Cl_2 (50 mL × 3) and the combined mixture was washed by water (20 mL × 2) and dried over Na_2SO_4, and then concentrated under reduced pressure. The residue was chromatographed on silica gel (Wako C-300, 500 g) using CH_2Cl_2 as eluents to give crude **5b** as a yellow powder. Recrystallisation from MeOH/$CHCl_3$ afforded 4,12,20-triacetylcalix[3]benzofuran **5b** (38 mg, 41 %) as a yellow powder. M.p. 242–243 °C. IR: ν_{max} (KBr)/cm^{-1}: 1675 (C=O), 1556, 1151. ^{1}H NMR (400 MHz, $CDCl_3$): δ = *cone*–2.64 (9H, s, -CO*CH*$_3$), 4.68 (3H, d, *J* = 13.6 Hz, *CH*$_2$), 4.99 (3H, d, *J* = 13.2 Hz, *CH*$_2$), 7.61 (3H, d, *J* = 8.8 Hz, Ar–*H*), 7.80 (6H, dd, *J* = 7.2 Hz, Ar–*H*), *saddle*–2.64 (9H, s, -CO*CH*$_3$), 4.58 (6H, s, *CH*$_2$) and 7.34 (9H, dd, *J* = 8.0 Hz, Ar–*H*) ppm. ^{13}C NMR (100 MHz, $CDCl_3$): δ = 31.07, 35.85, 117.45, 124.65, 134.77, 150.48, 159.97, 166.52 and 192.36 ppm. FABMS: *m/z*: 516.23 [M^+]. $C_{33}H_{24}O_6$ (516.16): calcd C 76.73, H 4.68; found: C 77.01, H 4.91.

Notes and references

[a]*Department of Applied Chemistry, Faculty of Science and Engineering, Saga University, Honjo-machi 1, Saga-shi, Saga 840-8502, Japan. Fax: (internat.) + 81(0)952/28-8548; E-mail: yamatot@cc.saga-u.ac.jp.*
[b]*Chemical Research Division, Bangladesh Council of Scientific and Industrial Research(BCSIR), Dhanmondi, Dhaka-1205, Bangladesh*
[c]*Institute for Materials Chemistry and Engineering, Kyushu University, 6-1, Kasugakoen, Kasuga 816-8580, Japan*
[d]*Department of Chemistry, Memorial University of Newfoundland, St. John's, Newfoundland and Labrador A1B 3X7, Canada*
[e]*School of Chemistry, University of East Anglia, Norwich, NR4 7TJ, UK*
[f]*Department of Chemistry, The University of Hull, Cottingham Road, Hull, Yorkshire, HU6 7RX, UK.*

† Electronic Supplementary Information (ESI) available: Details of the single-crystal X-ray crystallographic data and DFT computational data and xyz files. For ESI and crystallographic data in CIF see DOI: 10.1039/b000000x/

1. (*a*) J. Breitenbach, J. Boosfeld and F. Vogtle, *In Comprehensive Supramolecular Chemistry*; Vogtle, F., Ed.; Elsevier Science, 1996, **2**, 29–67; (*b*) T. Ogoshi, K. Kitajima, T. Aoki, S. Fujinami, T. Yamagishi and Y. Nakamoto, *J. Org. Chem.,* 2010, **75**, 3268–3273; (*c*) R. Zadmard and T. Schrader, *J. Am. Chem. Soc.*, 2005, **127**, 904–9015.
2. (*a*) F. Vogtle, *Cyclophane Chemistry*; Wiley: Chichester, 1993; (*b*) C. D. Gutsche, *Calixarenes: An Introduction; Royal Society of Chemistry: Cambridge*, 2008.
3. (*a*) R. Gleiter and H. Hopf, *Modern Cyclophane Chemistry*; Wiley-VCH Verlag GmbH & Co. KgaA.: Germany, 2004; (*b*) K. Yoon and K. Kim, *J. Org. Chem.*, 2005, **70**, 427–432; (*c*) T. Sawada, *In New Trends in Structural Organic Chemistry*; Takamura, H., Ed.; Research Signpost: Kerala, India, 2005, 85; (*d*). C. Talotta, N. A. De Simone, C. Gaeta and P. Neri, *Org. Lett.*, 2015, **17**, 1006–1009; (*e*) C. Gaeta, C. Talotta, L. Margarucci, A. Casapullo and P. Neri, *J. Org. Chem*., 2013, **78**, 7627–7638.
4. (*a*) S. Gentile, F. G. Gulino, D. Sciotto and C. Sgarlata, *Lett. Org. Chem*., 2006, **3**, 48–53; (*b*) D. Jokic, C. Boudon, G. Pognon, M. Bonin, K. J. Schenk, M. Gross and J. Weiss, *Chem. Eur. J.,* 2005, **11**, 4199–4209; (*c*) O. G. Barton, M. Schmidtmann, A. Mueller and J. Mattay, *New J. Chem.,* 2004, **28**, 1335–1339; (*d*) T. Sawada, M. Morita, K. Chifuku, Y. Kuwahara, H. Shosenji, M. Takafuji and H. Ihara, *Tetrahedron Lett.*, 2007, **48**, 9051–9055.
5. (*a*) D. Huh, K. L. Mills, X. Zhu, M. A. Burns, M. D. Thouless and S. Takayama, *Nature Mater.* 2007, **6**, 424–428; (*b*) R. Lin and J. A. Rogers, *Nano Lett.,* 2007, **7**, 1613–1621; (*c*) F. Jia, Z. He, L.-P. Yang, Z.-S. Pan, M. Yi, R.-W. Jiang and W. Jiang, *Chem. Sci*., 2015, **6**, 6731–6738; (*d*) F. Jia, H.-Y. Wang, D.-H. Li, L.-P. Yang and W. Jiang, *Chem. Commun.*, 2016, **52**, 5666–5669.
6. (*a*) J. J. Chambers, D. M. Kurrasch-Orbaugh, M. A. Parker and D. E. Nichols, *J. Med. Chem*., 2001, **44**, 1003–1010; (*b*) L. Rene, J.-P. Buisson, R. Royer and D. Averbeck, *Eur. J. Med. Chem.,* 1977, **12**, 31–34; (*c*) C. Bilger, P. Demerseman, J. P. Buisson, R. Royer, P. Gayral and J. Fourniat, *Eur. J. Med. Chem.,* 1987, **22**, 213–219; (*d*) K. S. K. Murthy, B. Rajitha, M. K. Rao, T. R. Komuraiah and S. M. Reddy, *Heterocycl. Commun.* 2002, **8**, 179–186.
7. (*a*) K. C. Nicolaou, S. A. Snyder, A. Bigot and J. A. Pfefferkora, *Angew. Chem., Int. Ed. Engl.,* 2000, **39**, 1093–1096; (*b*) J. Habermann, S. V. Ley and R. Smits*, J. Chem. Soc., Perkin Trans.1,* 1999, 2421–2423; (*c*) H. M. Meshram, K. C. Sekhar, Y. S. S. Ganesh and J. S. Yadav, *Synlett*., 2000, 1273–1274; (*d*) Z. Chen, X. Wang, W. Lu and J. Yu, *Synlett*, 1991, 121–122.
8. (*a*) K. K. Park, H. Seo, J.-G. Kim and I.-H. Suh, *Tetrahedron Lett*., 2000, **41**, 1393–1396; (*b*) K. K. Park, I. K. Han and J. W. Park, *J. Org. Chem.,* 2001, **66**, 6800–6802.
9. (*a*) A. R. Katritzky, Y. Ji, Y. Fang and I. Prakash, *J. Org. Chem*., 2001, **66**, 5613–5615; (*b*) X. Xie, B. Chen, J. Lu, J. Han, X. She and X. Pan, *Tetrahedron Lett.*, 2004, **45**, 6235–6237; (*c*) M. del Carmen Cruz and J. Tamariz, *Tetrahedron Lett.*, 2004, **45**, 2377–2380.
10. (*a*) I. Yavari, M. Anary-Abbasinejad and A. Alizadeh, *Tetrahedron Lett.*, 2002, **43**, 4503–4505; (*b*) M. Jorgensen, F. C. Krebs and K. J. Bechgaard, *Org. Chem.*, 2000, **65**, 8783–8785; (*c*) A. R. Katritzky, L. Serdyuk, L. Xie, *J. Chem. Soc., Perkin Trans. 1*, 1998, 1059–1064; (*d*) J. N. Chatterjea, V. N. Mehrotra and S. K. Roy, *Berichte.,* 1963, **96**, 1167–1176; (*e*) V. K. Mahesh, R. Sharma and M. Maheshwari, *Indian J. Chem.,* 1979, **17B**, 528–530.
11. (*a*) K. K. Park, H. Lim, S.-H. Kim and D. H. Bae, *J. Chem. Soc., Perkin Trans.1*, 2002, 310–314; (*b*) K. K. Park and H. Lim, *Heterocycles,* 2002, **57**, 657–664; (*c*) K. K. Park, S.-H. Kim and J. W. Park, *J. Photochem. Photobiol. A: Chem*. 2004, **163**, 241–247; (*d*) M. A. Aziz, J. V. Auping and M. A. Meador, *J. Org. Chem.,* 1995, **60**, 1303–1308.
12. (*a*) W.-C. Zhang and C.-J. Li, *Tetrahedron*, 2000, **56**, 2405–2411; (*b*) J. S. Yadav, B. V. S. Reddy, M. S. Reddy, N. Niranjan and A. R. Prasad, *Eur. J. Org. Chem.*, 2003, 1770–1783; (*c*) J. J. Jaber, K. Mitsui, S. D. Rychnovsky, *J. Org. Chem.,* 2001, **66**, 4679–4686; (*d*) G. Sabitha, K. B. Reddy, G. S. K. K. Reddy, N. Fatima, J. S. Yadav, *Synlett*, 2005, **15**, 2347–2351; (*e*) G. Sabitha, K. B. Reddy, M. Bhikshapathi and J. S. Yadav, *Tetrahedron Lett.,* 2006, **47**, 2807–2810.
13. (*a*) J. M. Van Gelder, J. Brenn, I. Thondorf and S. E. Biali, *J. Org. Chem.,* 1997, **62**, 3511–3519; (*b*) S. Simann, K. Agbaria and S. E. Biali, *J. Org. Chem.* 2002, **67**, 6136–6142.
14. (*a*) A. M. Litwak and S. E. Biali, *J. Org. Chem.*, 1992, **57**, 1943–1945; (*b*) O. Aleksiuk, F. Grynszpan and S. E. Biali, *J. Chem. Soc., Chem. Commun.,* 1993, 11–13; (*c*) A. M. Litwak, F. Grynszpan, O. Aleksiuk, S. Cohen and S. E Biali, *J. Org. Chem*. 1993, **58**, 393–402; (*d*) O. Aleksuik, F. Grynszpan and S. E. Biali, *J. Org. Chem.*, 1993, **58**, 1994–1996; (*e*) F. Grynszpan and S. E. Biali, *J. Chem. Soc., Chem. Commun.* 1994, 2545–2546; (*f*) F. Grynszpan, F. Aleksuik and S. E. Biali, *J. Org.Chem.,* 1994, **59**, 2070–2074.
15. (*a*) D. StC. Black, D. C. Craig, N. Kumar and R. Rezaie, *Tetrahedron*, 1999, **55**, 4803–4814; (*b*) D. StC. Black, D. C. Craig, N. Kumar and R. Rezaie, *Tetrahedron*, 2002, **58**, 5125–5134.
16. (*a*) C. D. Gutsche, *Calixarenes, Monographs in Supramolecular Chemistry*, **1**, Ed. J. Stoddard, The Royal Society of Chemistry, Cambridge, 1989; (*b*) J. Vicens and V. Böhmer (Eds.): *Calixarenes: A Versatile Class of Macrocyclic Compounds*, Kluwer Academic Publishers, Cambridge, 1990; (*c*) C. D. Gutsche, *Acc. Chem. Res.,* 1983, **16**, 161–170.

17. (*a*) K. Kim, S. J. Park and J.-I. Choe, *Bull. Korean Chem. Soc*., 2008, **29**, 1893–897; (*b*) J.-I. Choe and S.-K. Chang, *Bull. Korean Chem. Soc.,* 2002, **23**, 48–52; (*c*) J.-I. Choe and S. H. Lee, *Bull. Korean Chem. Soc.,* 2004, **25**, 553–556.
18. (*a*) M. M. Islam, T. Hirotsugu, P. Thuery, T. Matsumoto, J. Tanaka, M. R. J. Elsegood, C. Redshaw and T. Yamato, *J. Mol. Struct*., 2015, **1098**, 47–54; (*b*) M. M. Islam, T. Hirotsugu, T. Matsumoto, J. Tanaka, S. Rahman, P. E. Georghiou, C. Redshaw and T. Yamato, *Org. Biomol. Chem.*, 2015, **13**, 9055–9064.
19. (*a*) K. Tazoe, X. Feng, B. Sharma, S. Miyamoto and T. Yamato, *Can. J. Chem*., 2012, **90**, 222–229; (*b*) T. Yamato, L. K. Doamekpor and H. Tsuzuki, *Liebigs Ann.*, 1997, 1537–1544; (*c*) T. Yamato, L. K. Doamekpor, K. Koizumi, K. Kishi, M. Haraguchi and M. Tashiro, *Liebigs Ann*., 1995, **7**, 1259–1267; (*d*) L. K. Doamekpor, V. K. Nartey, R. K. Klake, T. Yamato, *International J. Org. Chem.,* 2012, **2**, 152–158; (*e*) T. Yamato, Y. Saruwataria, M. Yasumatsua and S. Ide, *Eur. J. Org. Chem.* 1998, 309–316; (*f*) T. Yamato and F. Zhang, *J. Incl. Phenom. Macrocyclic Chem.,* 2001, **39**, 55–64; (*g*) M. Tashiro and T. Yamato, *J. Org. Chem.* 1981, **46**, 1543–1552.
20. (*a*) T. Sawada, T. Hongo, N. Matsuo, M. Konishi, T. Kawaguchi and H. Ihara, *Tetrahedron*, 2011, **67**, 4716–4722; (*b*) T. Sawada, Y. Nishiyama, W. Tabuchi, M. Ishikawa, E. Tsutsumi, Y. Kuwahara and H. Shosenji, *Org. Lett.,* 2006, **8**, 1995–1997.
21. (*a*) T. Yamato, J. Matsumoto, M. Kajihara and M. Tashiro, *Chem. Express,* 1990, **5**, 769–772; (*b*) T. Yamato, J. Matsumoto, S. Ide, K. Tokuhisa, K. Suehiro and M. Tashiro, *J. Org. Chem.,* 1992, **57**, 5243–5246; (*c*) T. Yamato, J. Matsumoto, K. Tokuhisa, M. Kajihara, K. Suehiro and M. Tashiro, *Chem. Ber.,* 1992, **125**, 2443–2454; (*d*) M. M. Islam, T. Hirotsugu, T. Matsumoto, J. Tanaka and T. Yamato, *Can. J. Chem.* 2015, **93**, 1161–1168.
22. Initial molecular modeling calculations using the MMFF94 were performed using the PC Spartan'10 software from Wavefunction Inc., Irvine CA.
23. M. J. Frisch, G. W. Trucks, H. B. Schlegel, G. E. Scuseria, M. A. Robb, J. R. Cheeseman, G. Scalmani, V. Barone, B. Mennucci, G. A. Petersson, H. Nakatsuji, M. Caricato, X. Li, H. P. Hratchian, A. F. Izmaylov, J. Bloino, G. Zheng, J. L. Sonnenberg, M. Hada, M. Ehara, K. Toyota, R. Fukuda, J. Hasegawa, M. Ishida, T. Nakajima, Y. Honda, O. Kitao, H. Nakai, T. Vreven, Jr. J. A. Montgomery, J. E. Peralta, F. Ogliaro, M. Bearpark, J. J. Heyd, E. Brothers, K. N. Kudin, V. N. Staroverov, T. Keith, R. Kobayashi, J. Normand, K. Raghavachari, A. Rendell, J. C. Burant, S. S. Iyengar, J. Tomasi, M. Cossi, N. Rega, J. M. Millam, M. Klene, J. E. Knox, J. B. Cross, V. Bakken, C. Adamo, J. Jaramillo, R. Gomperts, R. E. Stratmann, O. Yazyev, A. J. Austin, R. Cammi, C. Pomelli, J. W. Ochterski, R. L. Martin, K. Morokuma, V. G. Zakrzewski, G. A. Voth, P. Salvador, J. J. Dannenberg, S. Dapprich, A. D. Daniels, O. Farkas, J. B. Foresman, J. V. Ortiz, J. Cioslowski and D. J. Fox, *Gaussian 09, Revision D.01*; Gaussian, Inc., Wallingford CT, 2013.

Synthesis, structural properties, electrophilic substitution reactions and DFT computational studies of calix[3]benzofurans

Md. Monarul Islam,[a,b] Thamina Akther,[a] Yusuke Ikejiri,[a] Taisuke Matsumoto,[c] Junji Tanaka,[c] Shofiur Rahman,[d] Paris E. Georghiou,[d] David L. Hughes,[e] Carl Redshaw[f] and Takehiko Yamato*[a]

[a]*Department of Applied Chemistry, Faculty of Science and Engineering, Saga University, Honjo-machi 1, Saga-shi, Saga 840-8502, Japan. Fax: (internat.) + 81(0)952/28-8548; E-mail: yamatot@cc.saga-u.ac.jp.*
[b]*Chemical Research Division, Bangladesh Council of Scientific and Industrial Research(BCSIR), Dhanmondi, Dhaka-1205, Bangladesh*
[c]*Institute for Materials Chemistry and Engineering, Kyushu University, 6-1, Kasugakoen, Kasuga 816-8580, Japan*
[d]*Department of Chemistry, Memorial University of Newfoundland, St. John's, Newfoundland and Labrador A1B 3X7, Canada*
[e]*School of Chemistry, University of East Anglia, Norwich, NR4 7TJ, UK*
[f]*Department of Chemistry, The University of Hull, Cottingham Road, Hull, Yorkshire, HU6 7RX, UK.*

Synthesis of highly flexible calix[3]benzofurans; effects of substituent groups on calix[3]benzofuran conformations were studied by DFT computational methods.

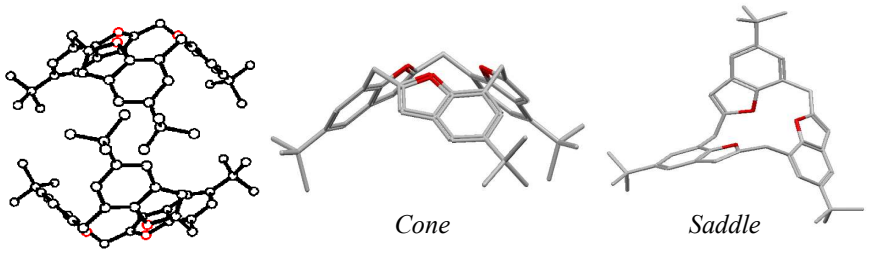

ELECTRONIC SUPPLEMENTARY INFORMATION

Manuscript title: **Synthesis, structural properties, electrophilic substitution reactions and DFT computational studies of calix[3]benzofurans**

Author(s): Md. Monarul Islam,[a,b] Thamina Akther,[a] Yusuke Ikejiri,[a] Taisuke Matsumoto,[c] Junji Tanaka,[c] Shofiur Rahman,[d] Paris E. Georghiou,[d] David L. Hughes,[e] Carl Redshaw[f] and Takehiko Yamato*[a]

[a]*Department of Applied Chemistry, Faculty of Science and Engineering, Saga University, Honjo-machi 1, Saga-shi, Saga 840-8502, Japan. Fax: (internat.) + 81(0)952/28-8548; E-mail: yamatot@cc.saga-u.ac.jp*
[b]*Chemical Research Division, Bangladesh Council of Scientific and Industrial Research(BCSIR), Dhanmondi, Dhaka-1205, Bangladesh.*
[c]*Institute of Material Chemistry and Engineering, Kyushu University, 6-1, Kasugakoen, Kasuga 816-8580, Japan*
[d]*Department of Chemistry, Memorial University of Newfoundland, St. John's, Newfoundland and Labrador A1B 3X7, Canada*
[e]*School of Chemistry, University of East Anglia, Norwich, NR4 7TJ, UK*
[f]*Department of Chemistry, The University of Hull, Cottingham Road, Hull, Yorkshire, HU6 7RX, UK.*

Table of Contents

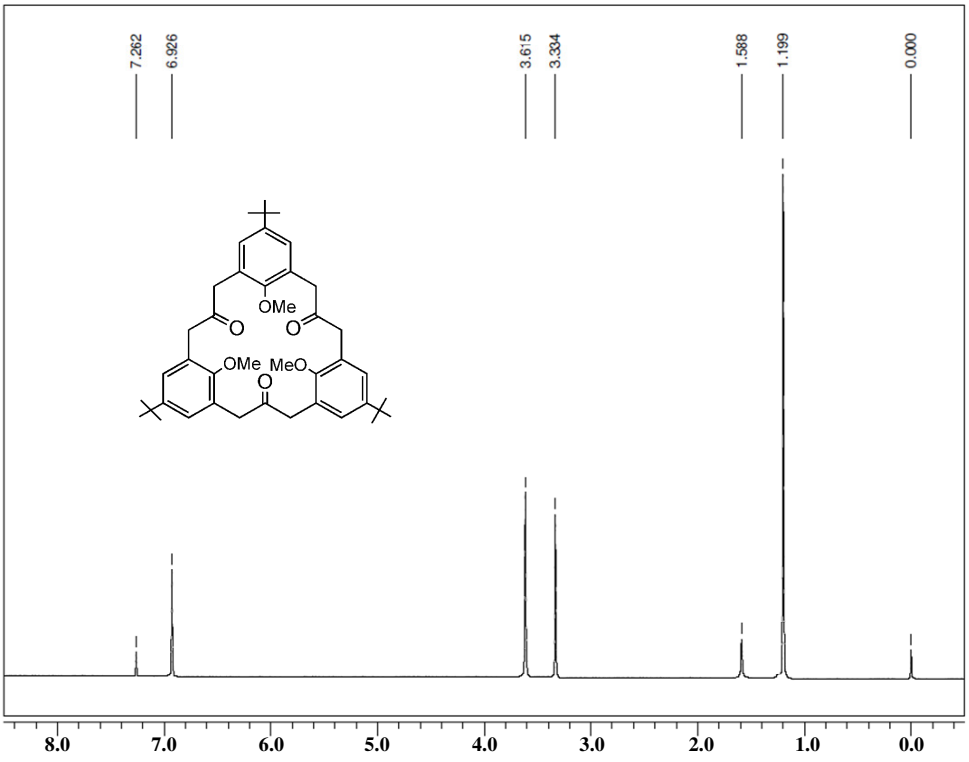

Figure S1. ^{1}H-NMR spectrum (400 MHz, 298 K, *$CDCl_3$) of the compound **2a.**

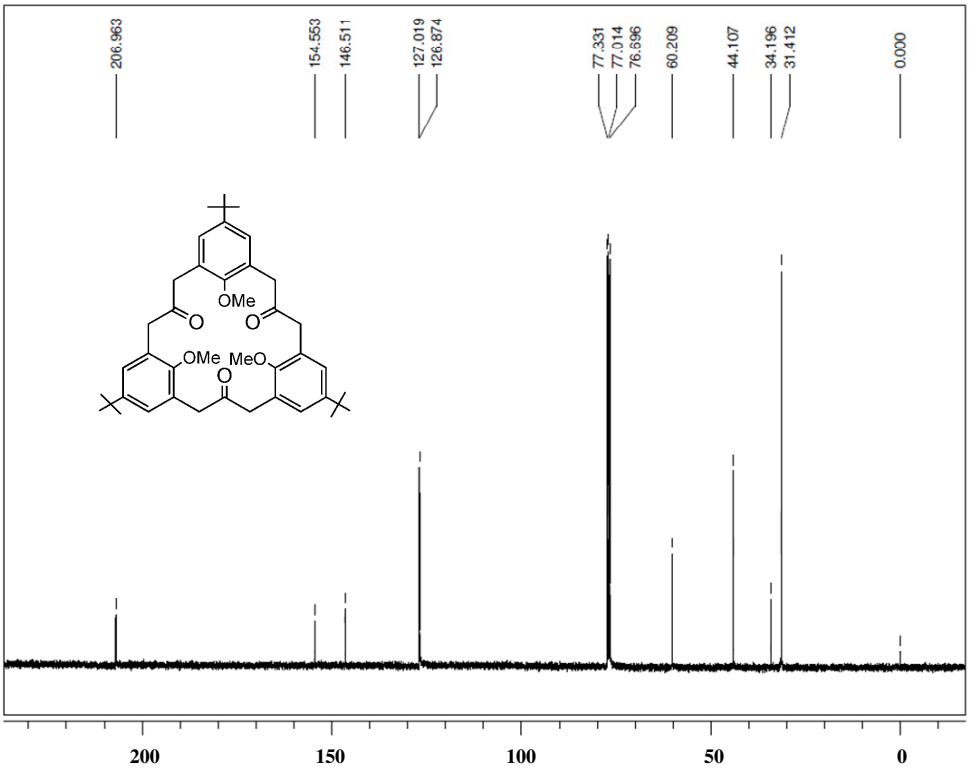

Figure S2: ^{13}C-NMR spectrum (100 MHz, 298 K, *$CDCl_3$) of the compound **2a.**

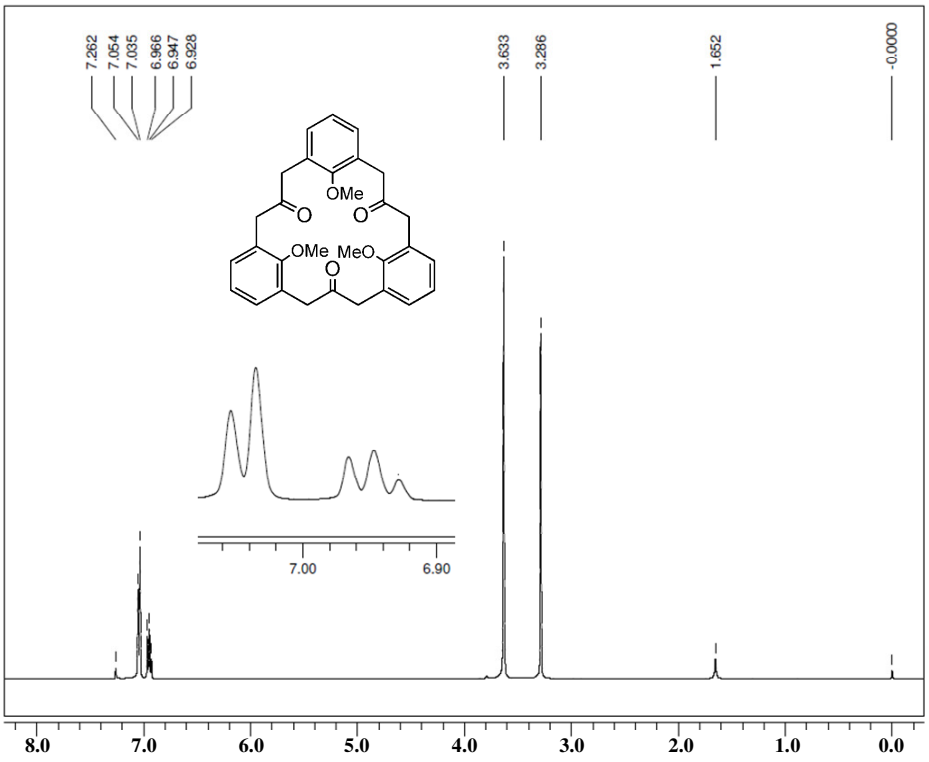

Figure S3: ^{1}H-NMR spectrum (400 MHz, 298 K, *$CDCl_3$) of the compound **2b.**

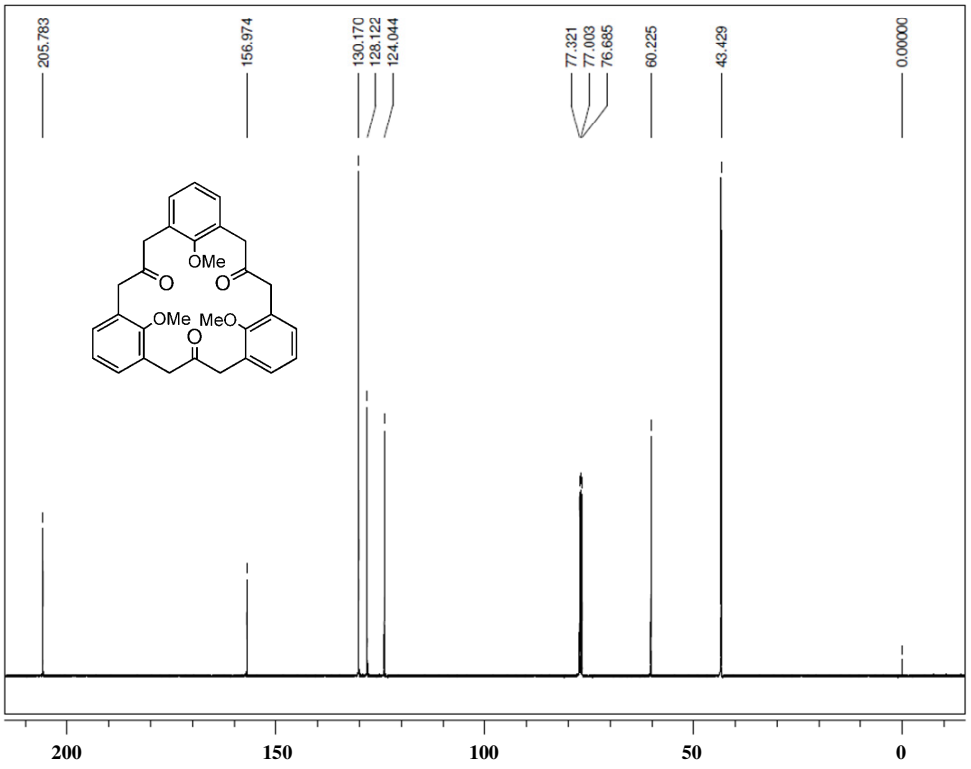

Figure S4: ^{13}C-NMR spectrum (100 MHz, 298 K, ⁎$CDCl_3$) of the compound **2b**.

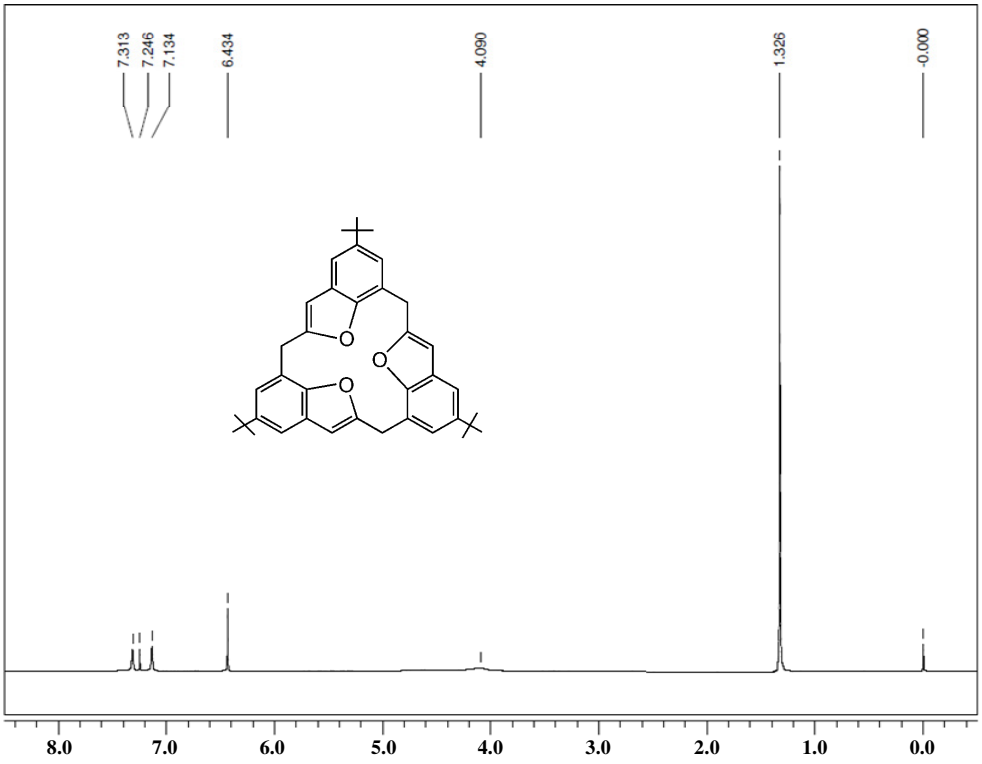

Figure S5: ^{1}H-NMR spectrum (400 MHz, 298 K, *$CDCl_3$) of the compound **4a.**

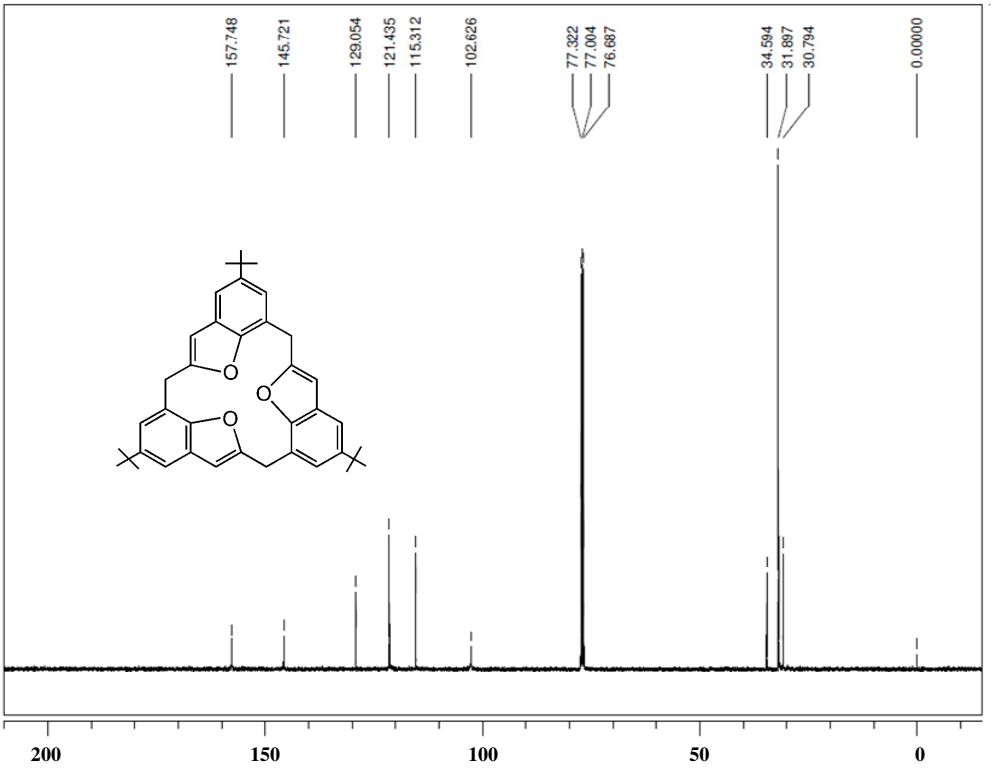

Figure S6: ^{13}C-NMR spectrum (100 MHz, 298 K, *$CDCl_3$) of the compound **4a.**

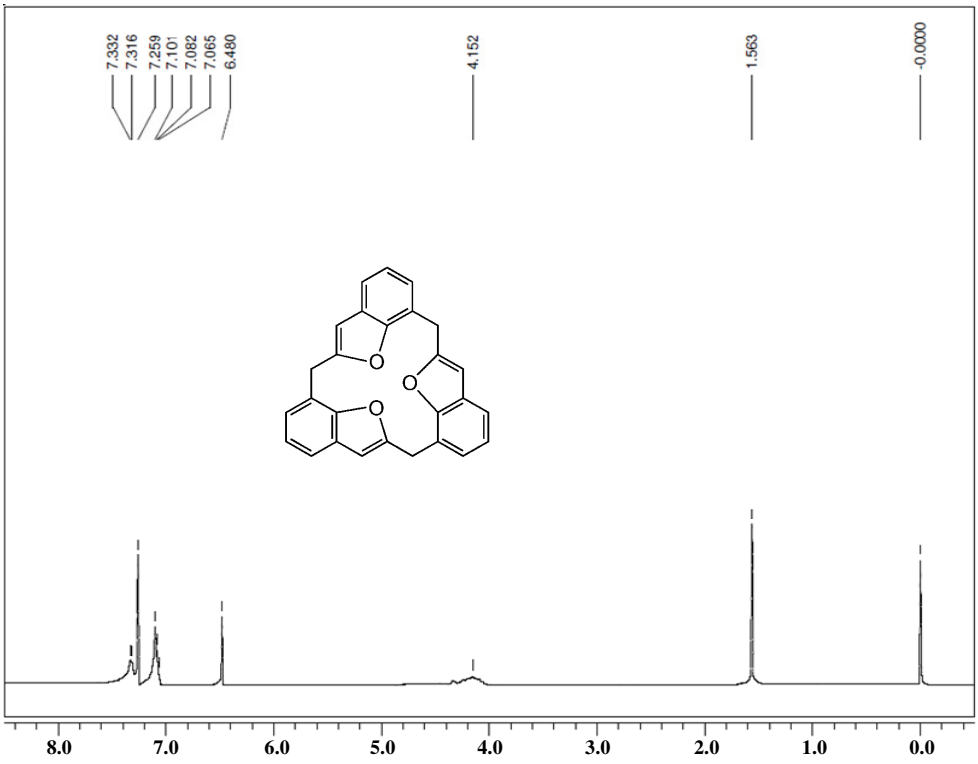

Figure S7: ^{1}H-NMR spectrum (400 MHz, 298 K, *$CDCl_3$) of the compound **5a.**

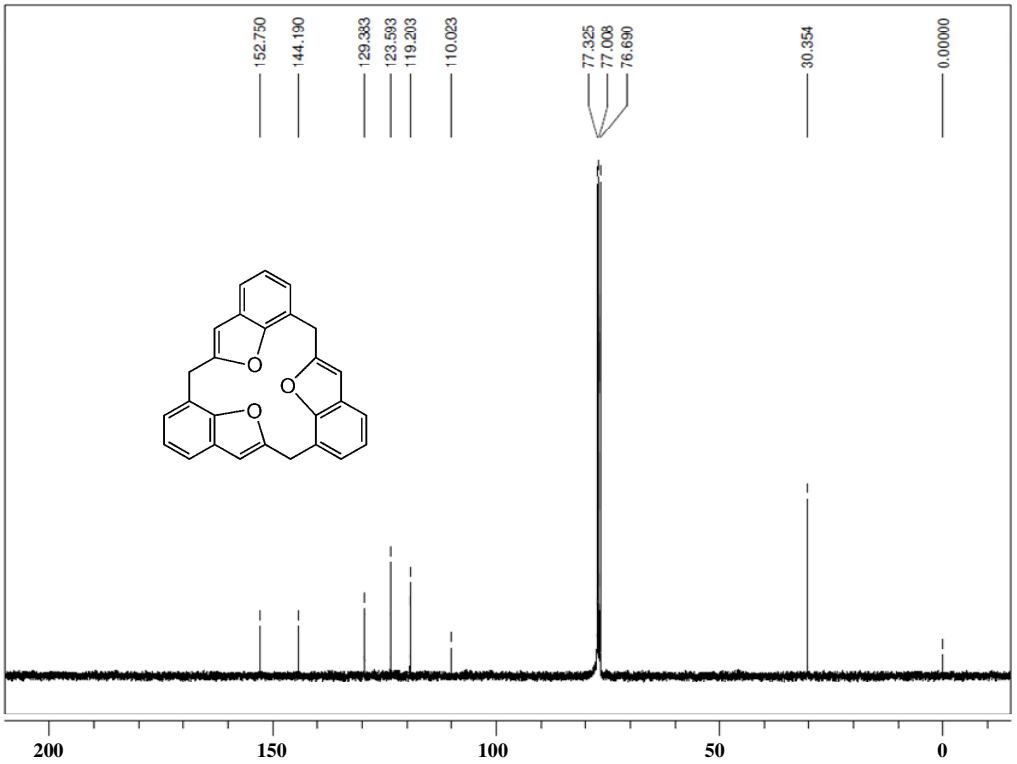

Figure S8: ^{13}C-NMR spectrum (100 MHz, 298 K, ⁎$CDCl_3$) of the compound **5a.**

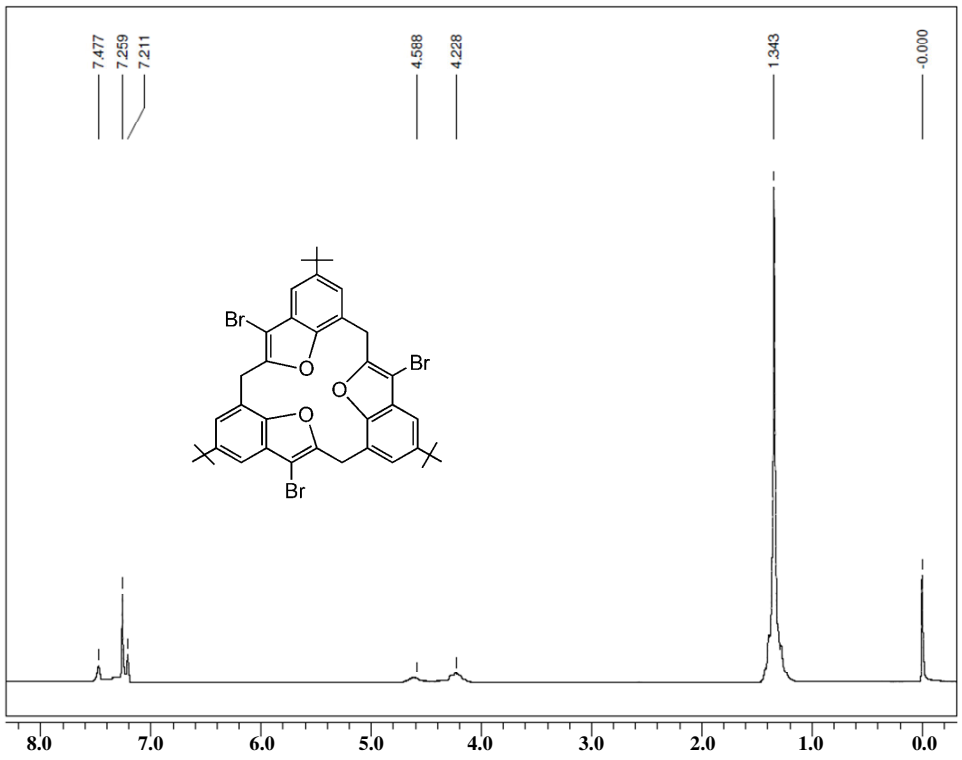

Figure S9: ^{1}H-NMR spectrum (400 MHz, 298 K, *$CDCl_3$) of the compound **4b.**

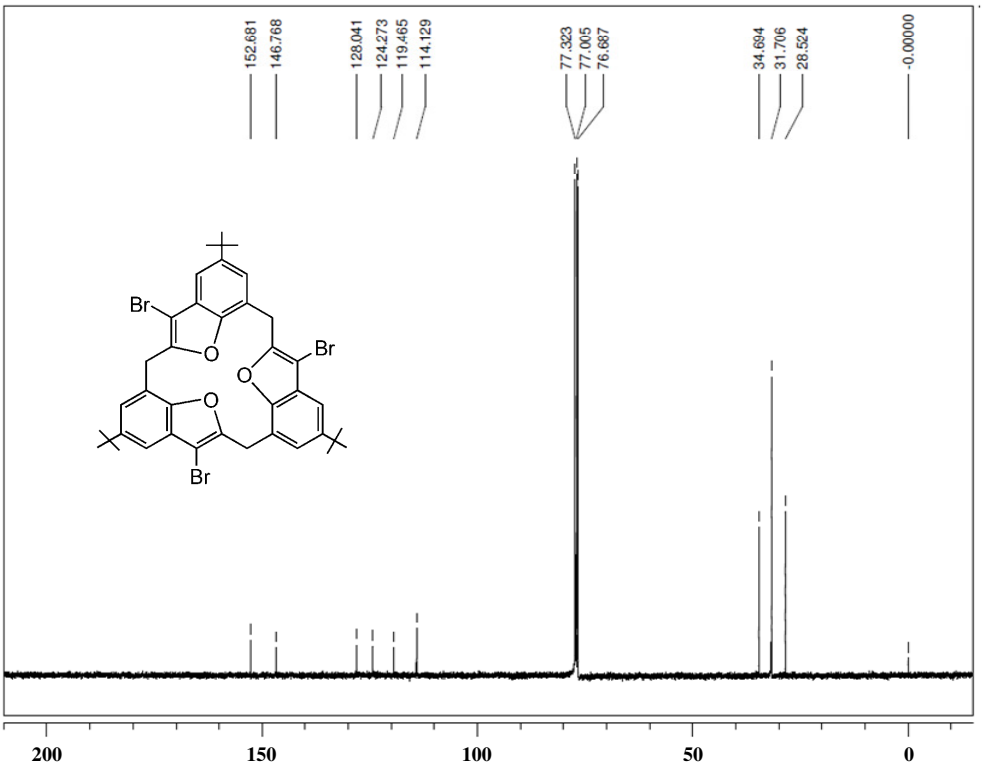

Figure S10: ^{13}C-NMR spectrum (100 MHz, 298 K, *$CDCl_3$) of the compound **4b.**

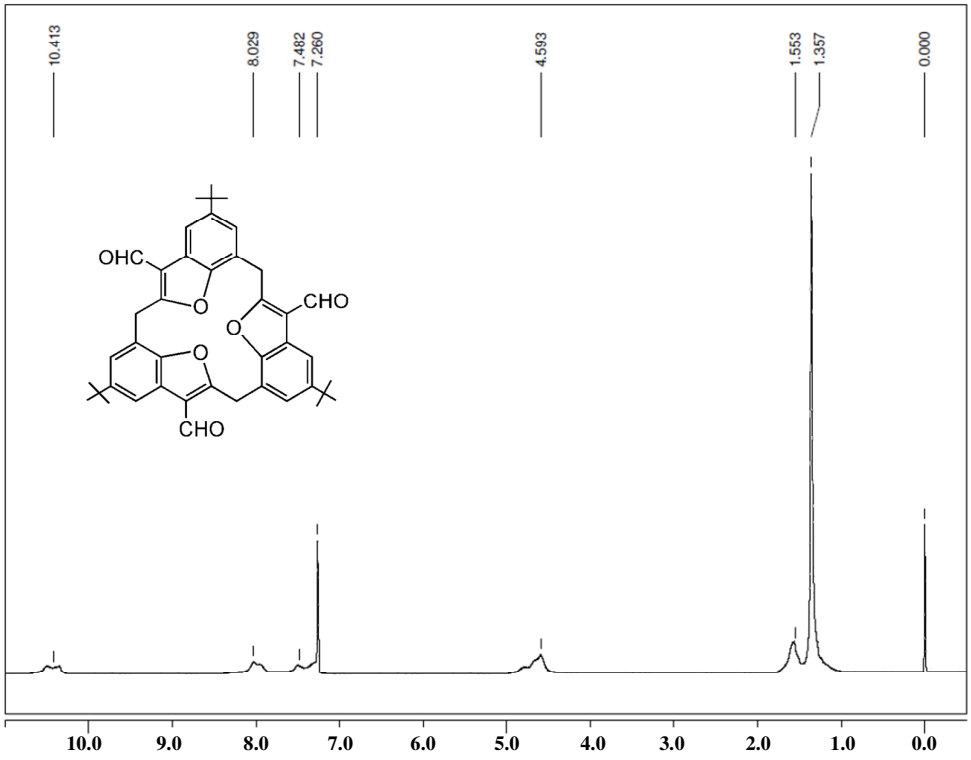

Figure S11: ^{1}H-NMR spectrum (400 MHz, 298 K, *$CDCl_3$) of the compound **4c.**

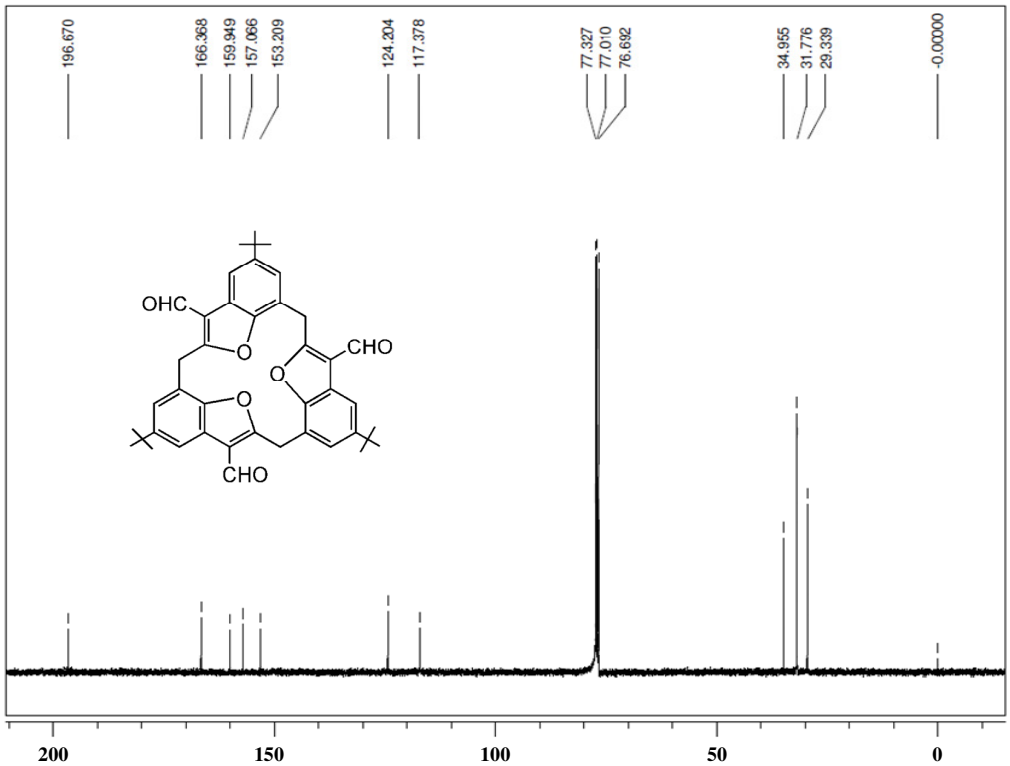

Figure S12: ^{13}C-NMR spectrum (100 MHz, 298 K, *$CDCl_3$) of the compound **4c.**

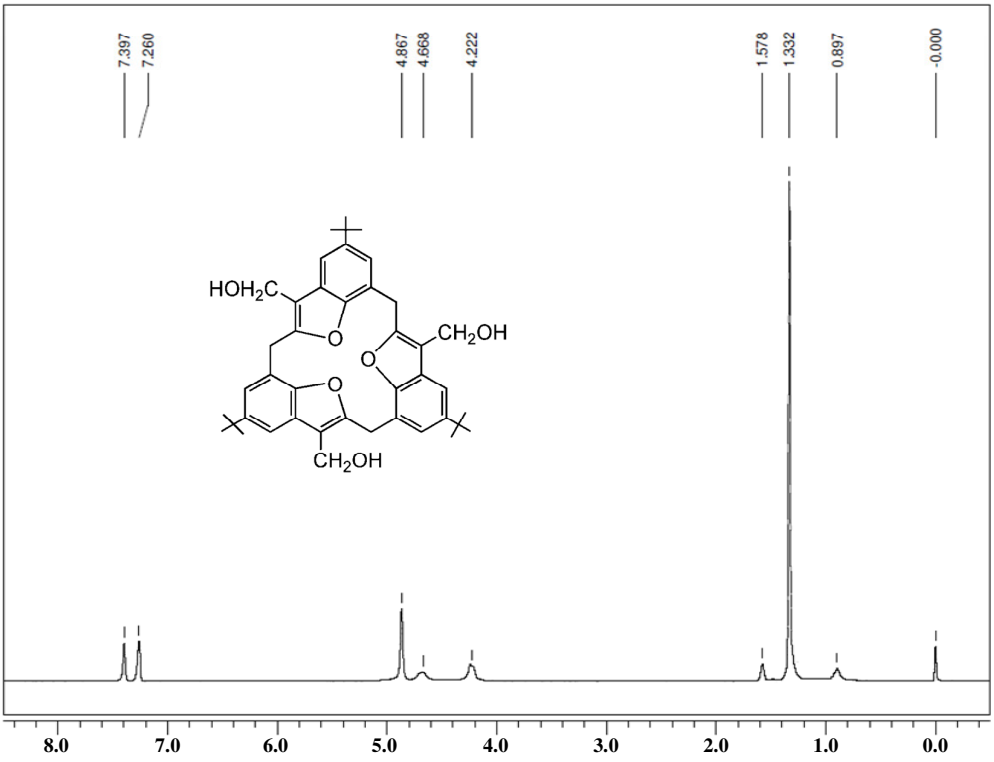

Figure S13: ^{1}H-NMR spectrum (400 MHz, 298 K, *$CDCl_3$) of the compound **4d.**

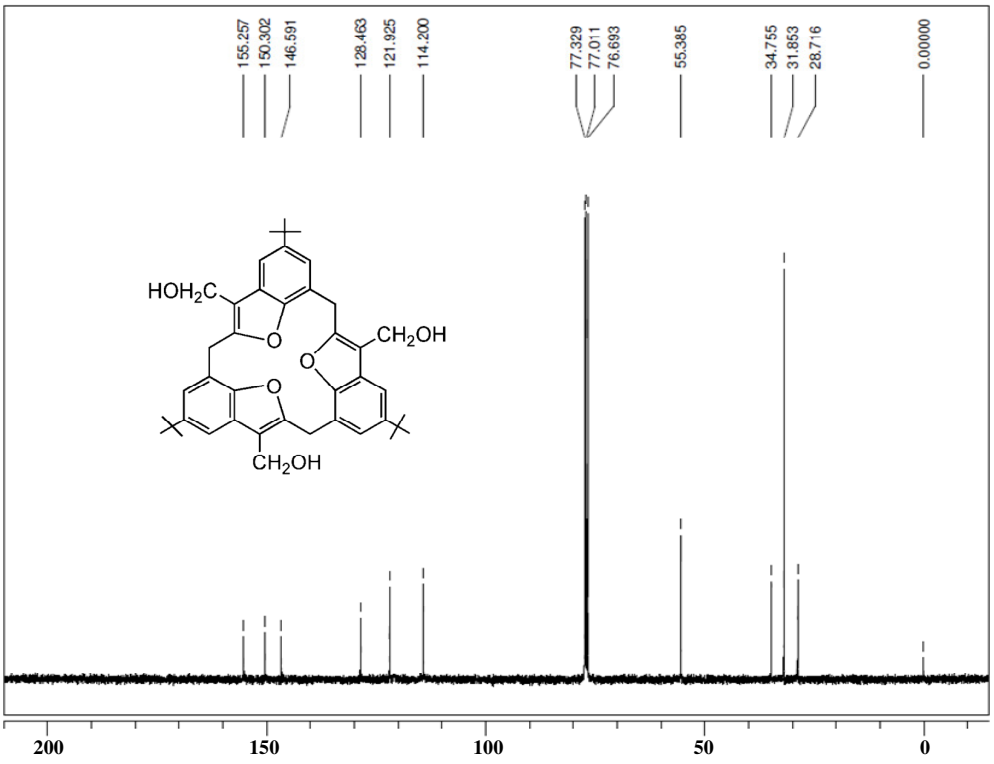

Figure S14: ^{13}C-NMR spectrum (100 MHz, 298 K, ∗$CDCl_3$) for the compound **4d.**

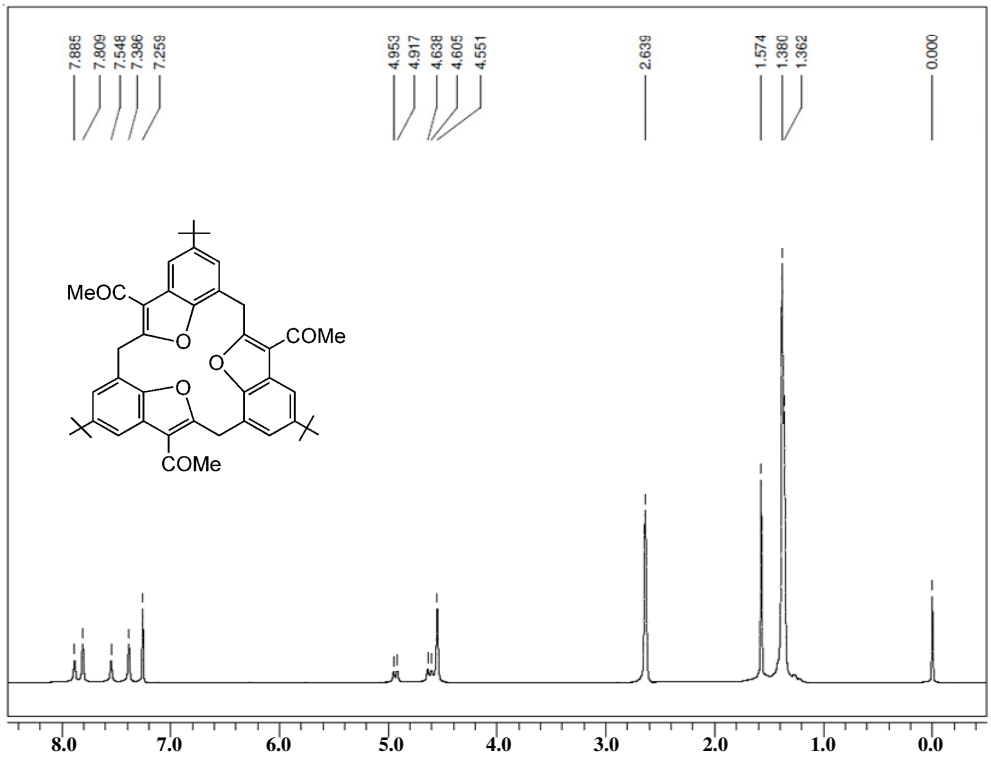

Figure S15: ^{1}H-NMR spectrum (400 MHz, 298 K, *$CDCl_3$) of the compound **4e.**

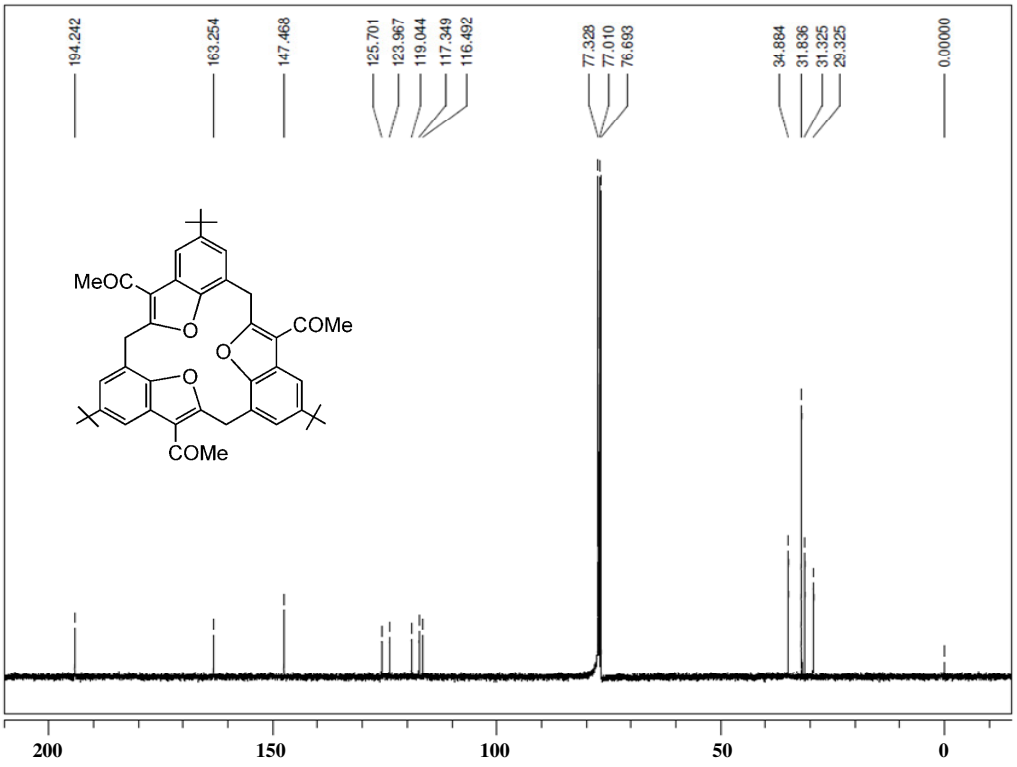

Figure S16: ^{13}C-NMR spectrum (100 MHz, 298 K, *$CDCl_3$) for the compound **4e.**

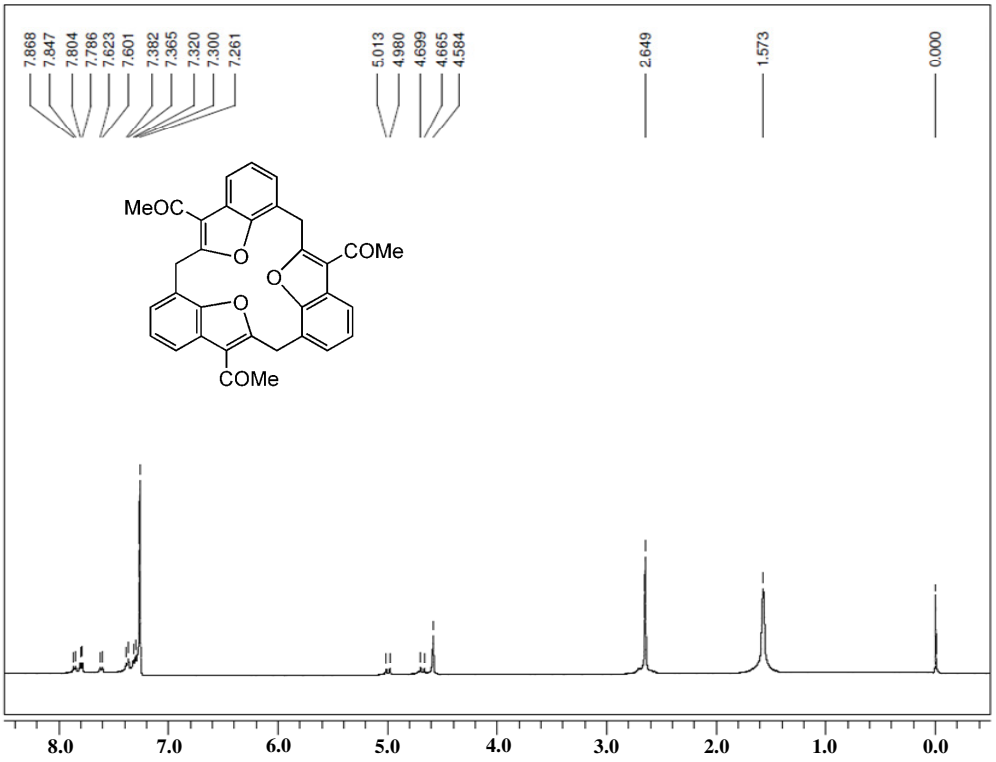

Figure S17: ^{1}H-NMR spectrum (400 MHz, 298 K, *$CDCl_3$) of the compound **5b**.

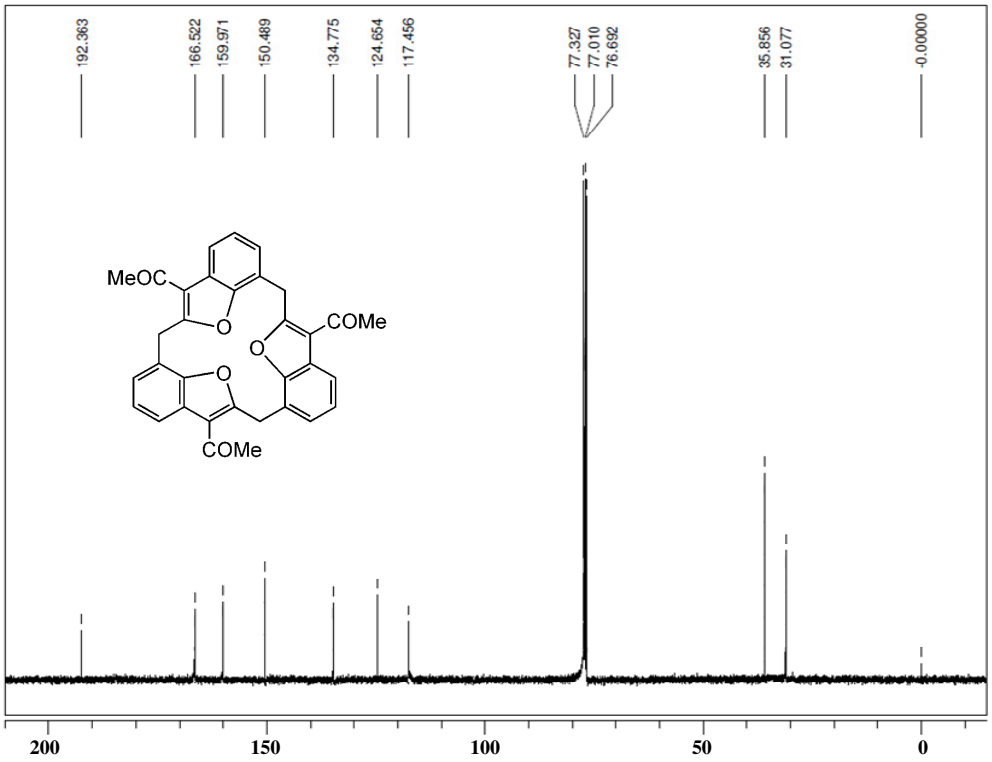

Figure S18: ^{13}C-NMR spectrum (100 MHz, 298 K, *$CDCl_3$) of the compound **5b**.

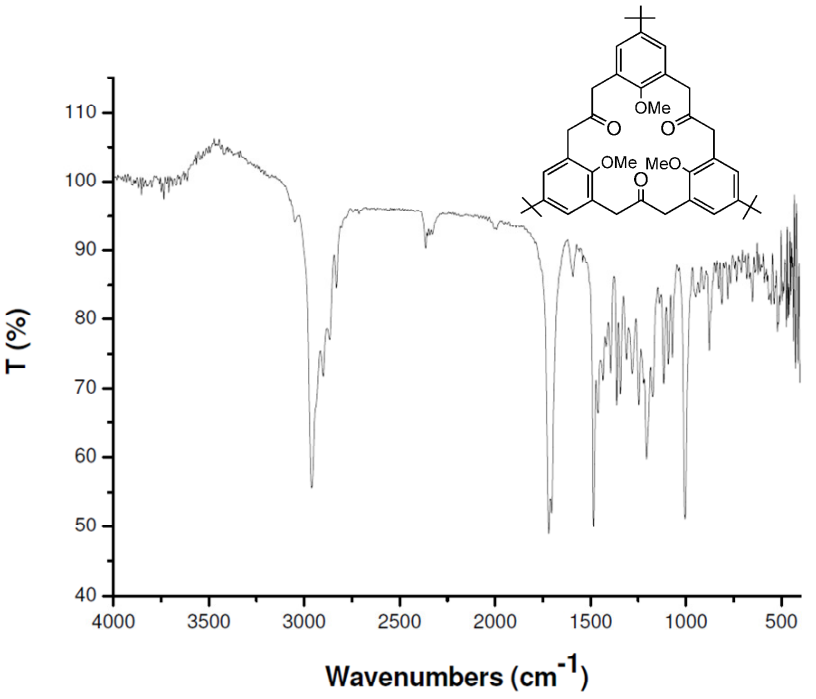

Figure S19: FT-IR spectrum of the compound **2a.**

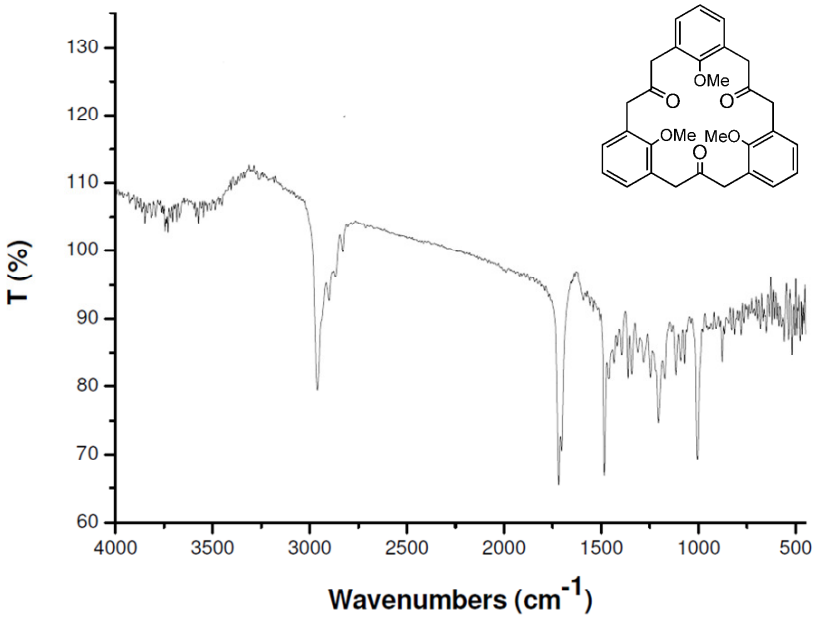

Figure S20: FT-IR spectrum of the compound **2b.**

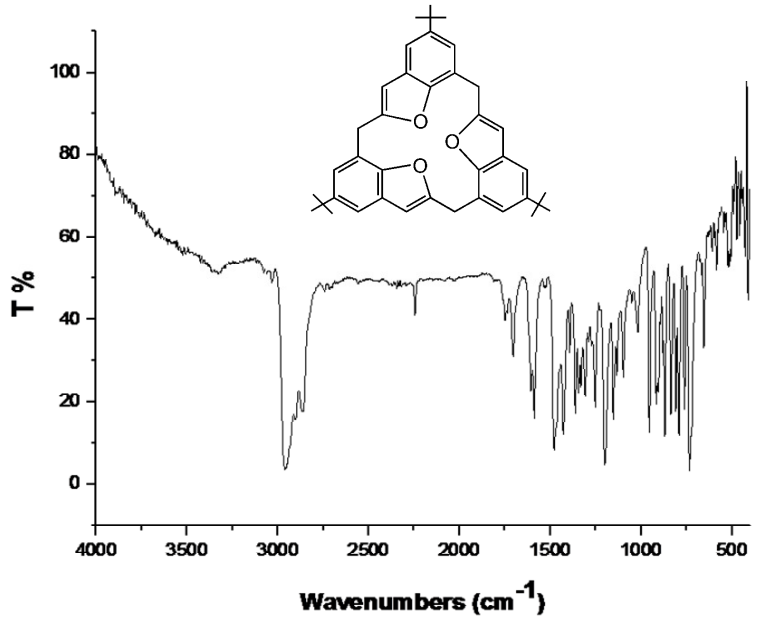

Figure S21: FT-IR spectrum of the compound **4a.**

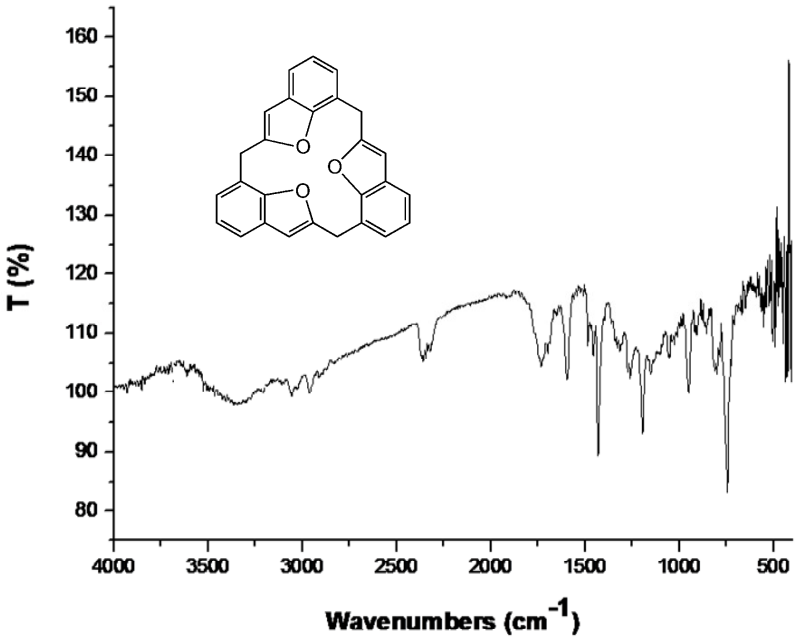

Figure S22: FT-IR spectrum of the compound **5a.**

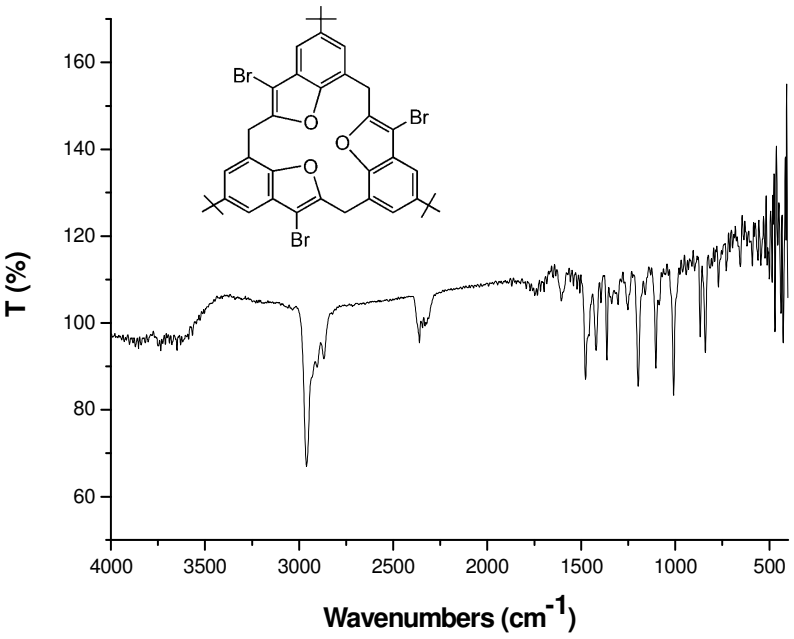

Figure S23: FT-IR spectrum of the compound **4b.**

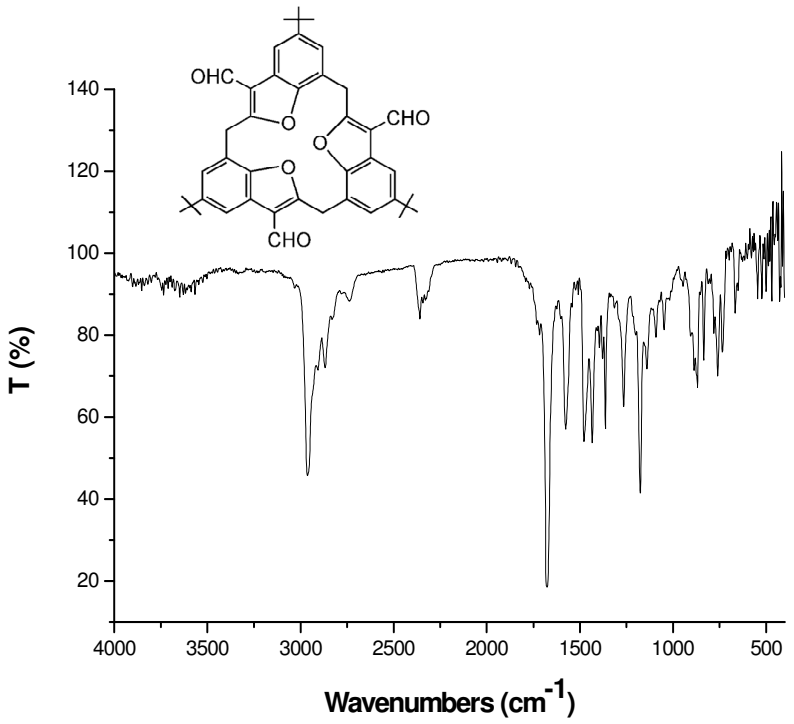

Figure S24: FT-IR spectrum of the compound **4c.**

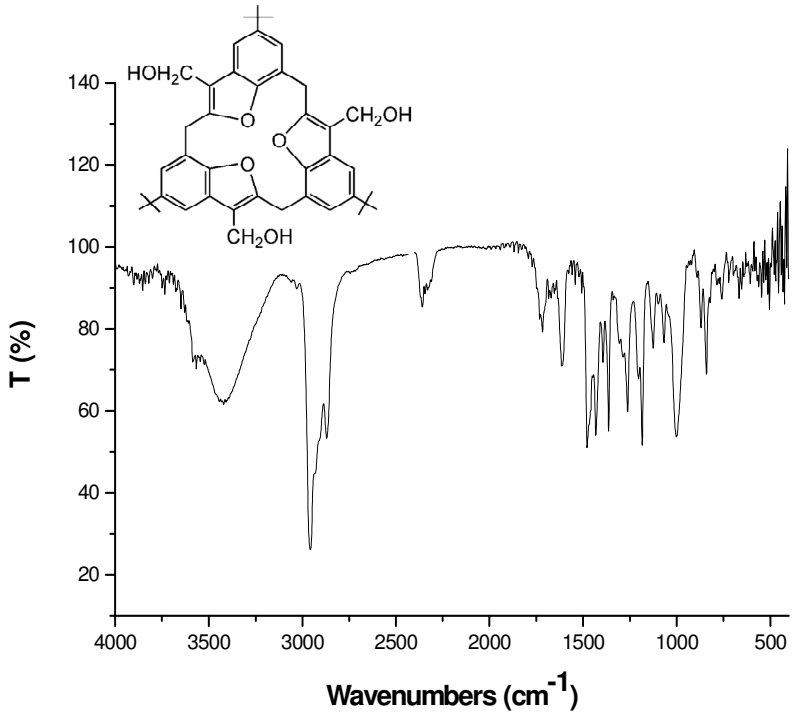

Figure S25: FT-IR spectrum of the compound **4d.**

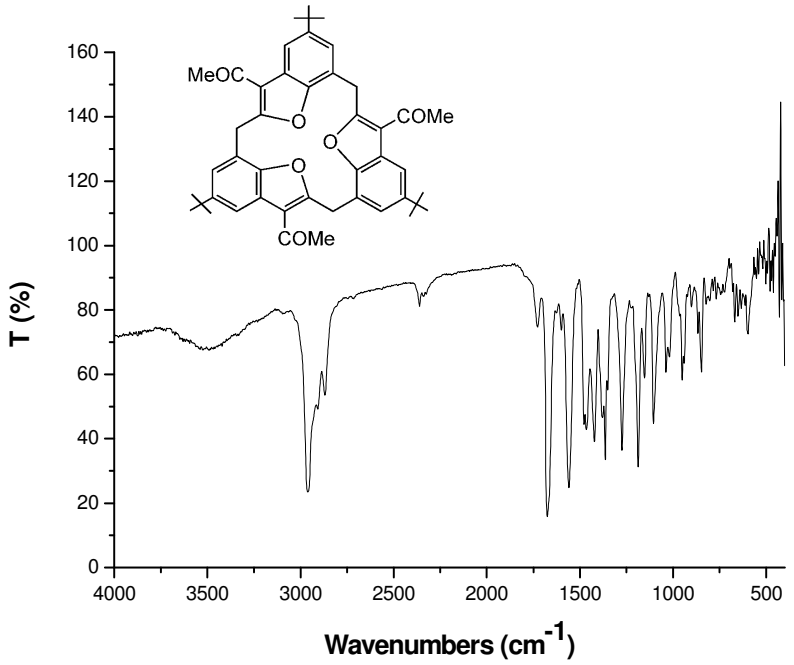

Figure S26: FT-IR spectrum of the compound **4e.**

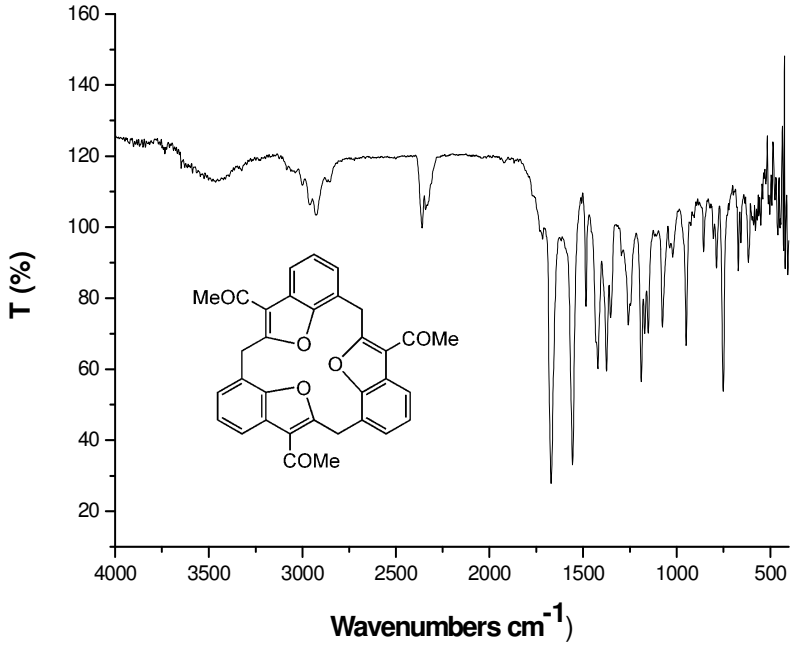

Figure S27: FT-IR spectrum of the compound **5b.**

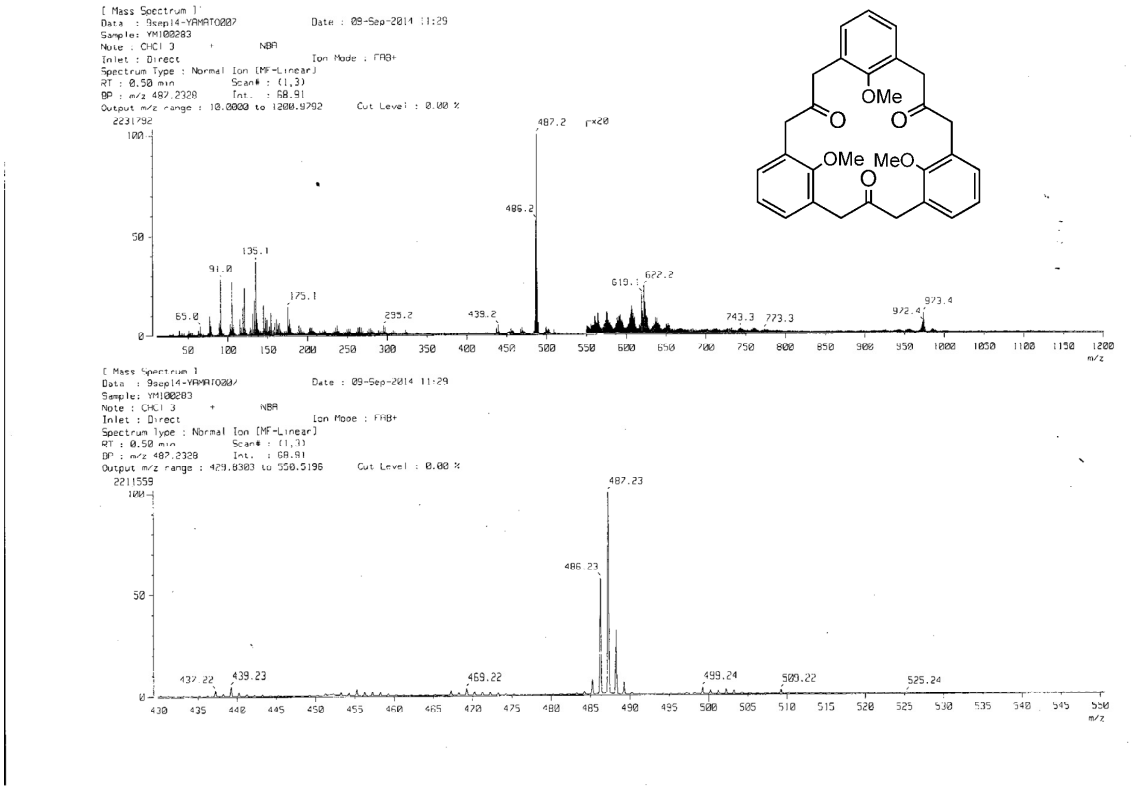

Figure S28: Mass-spectrum of the compound **2b**.

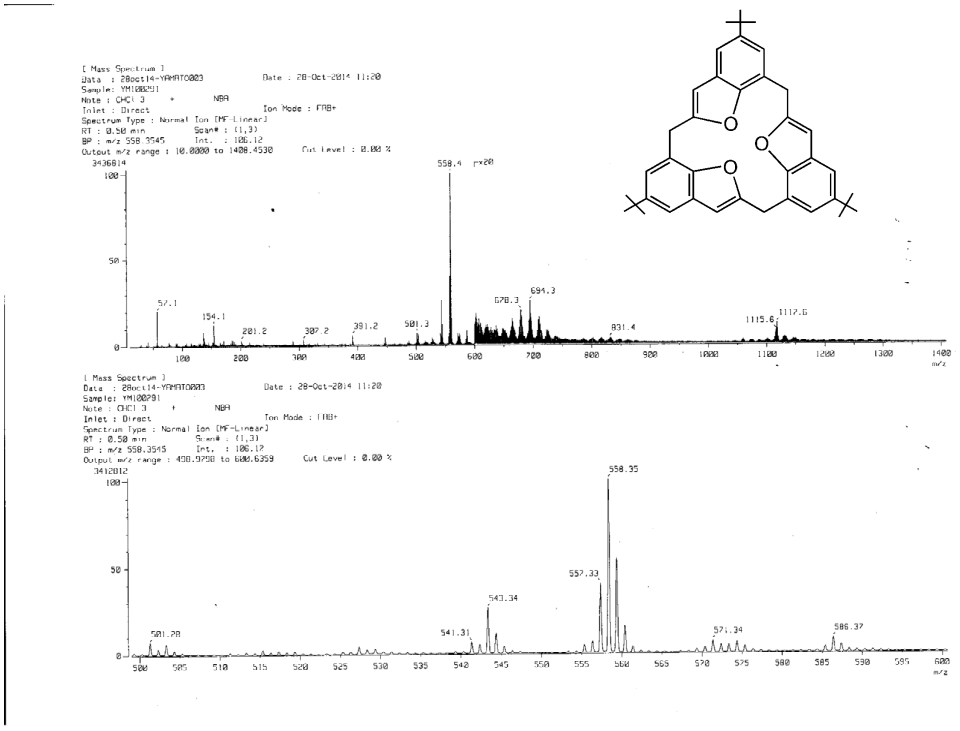

Figure S29: Mass-spectrum of the compound **4a**.

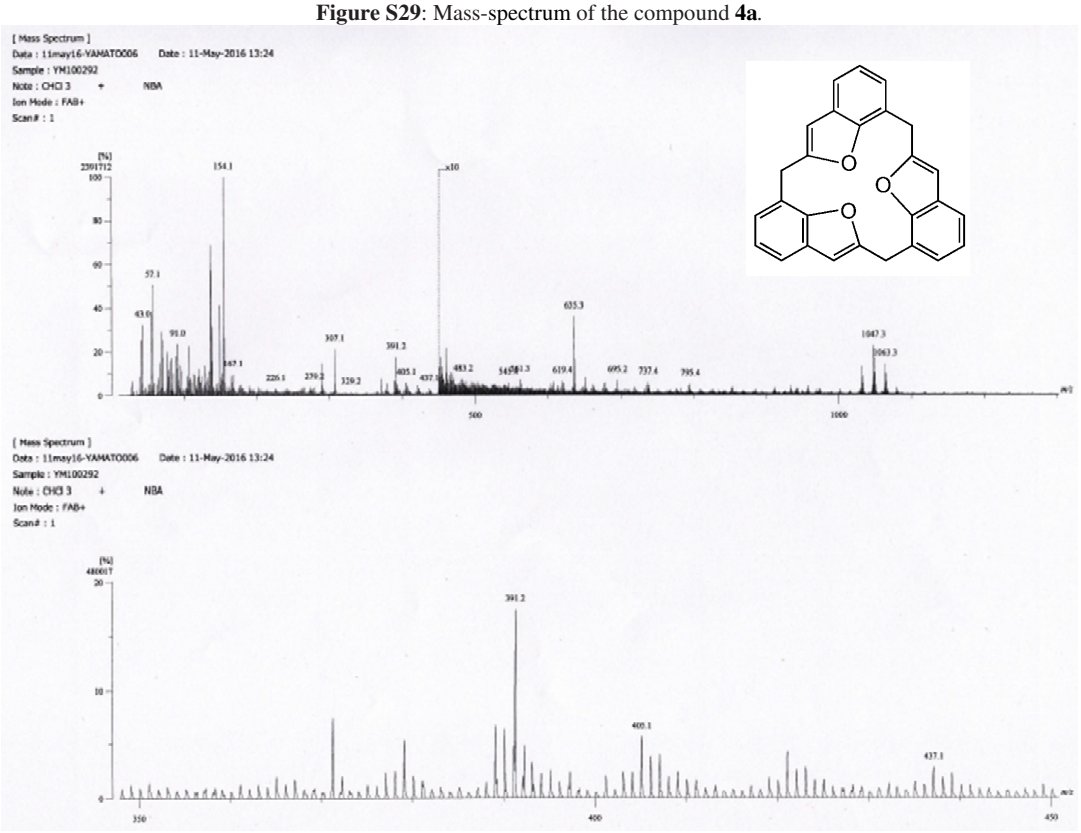

Figure S30: High resolution Mass-spectrum of the compound **5a**.

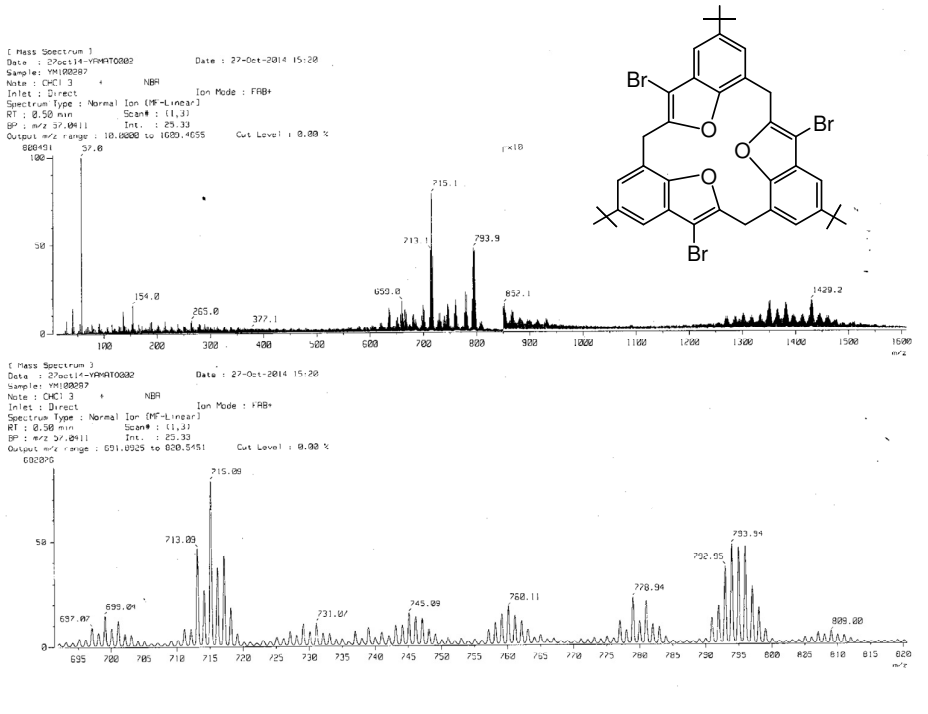

Figure S31: Mass-spectrum of the compound **4b**.

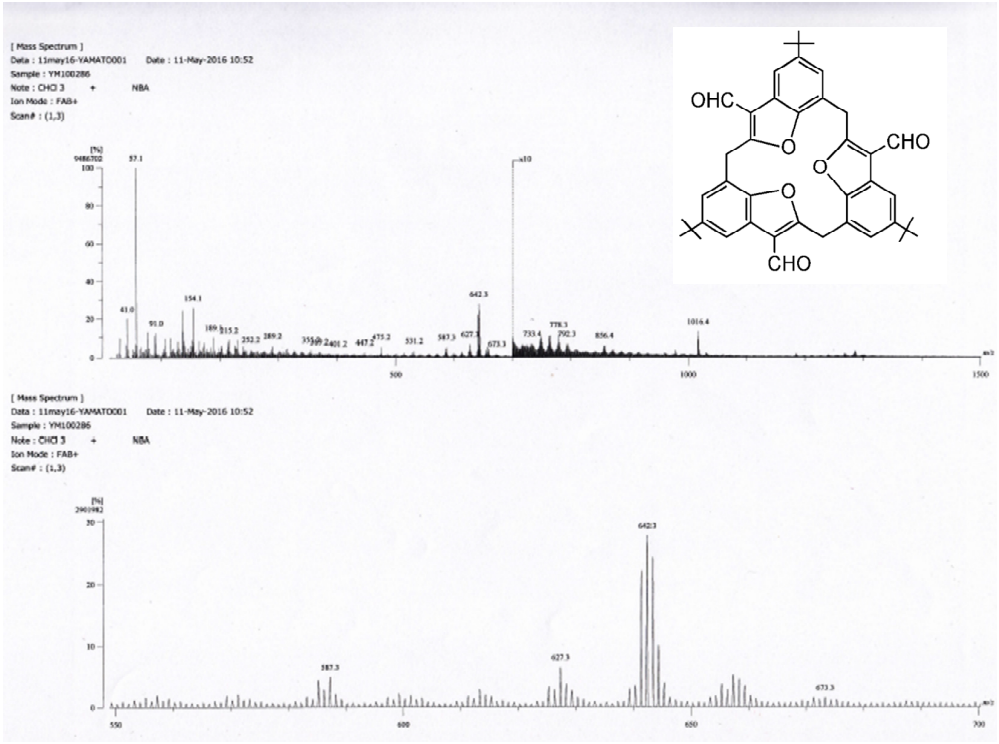

Figure S32: High resolution Mass-spectrum of the compound **4c**.

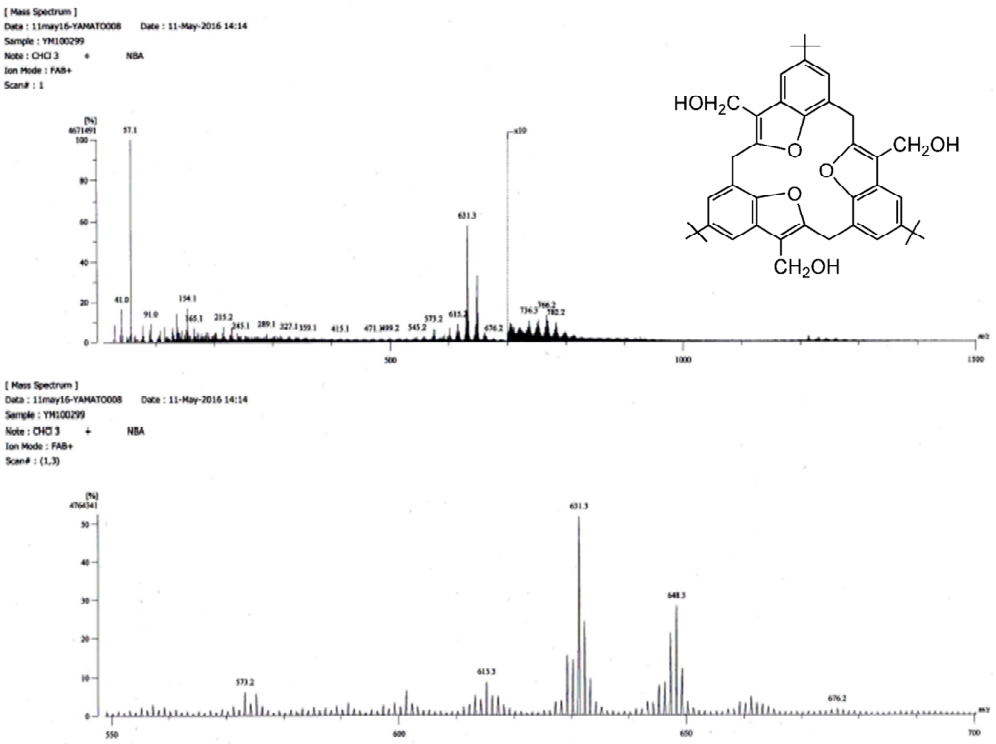

Figure S33: High resolution Mass-spectrum of the compound **4d**.

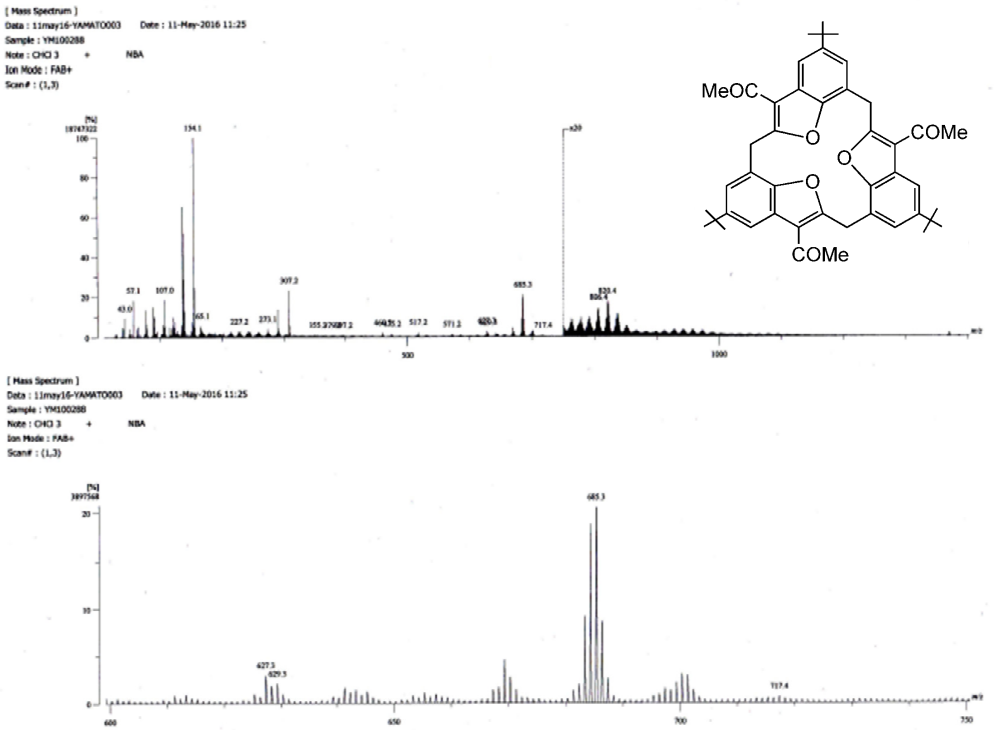

Figure S34: High resolution Mass-spectrum of the compound **4e**.

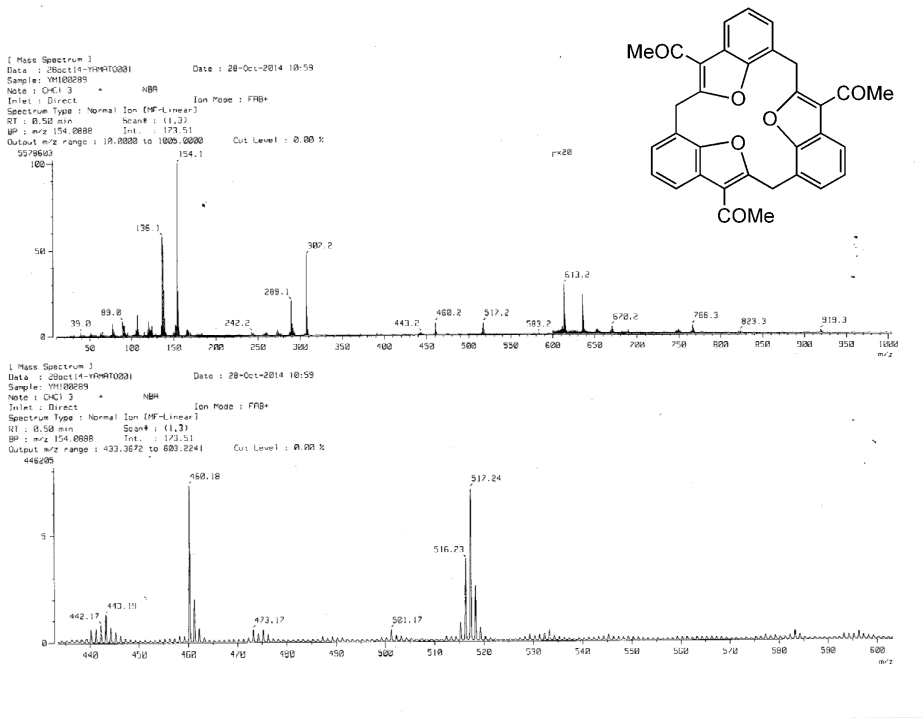

Figure S35: Mass-spectrum of the compound **5b**.

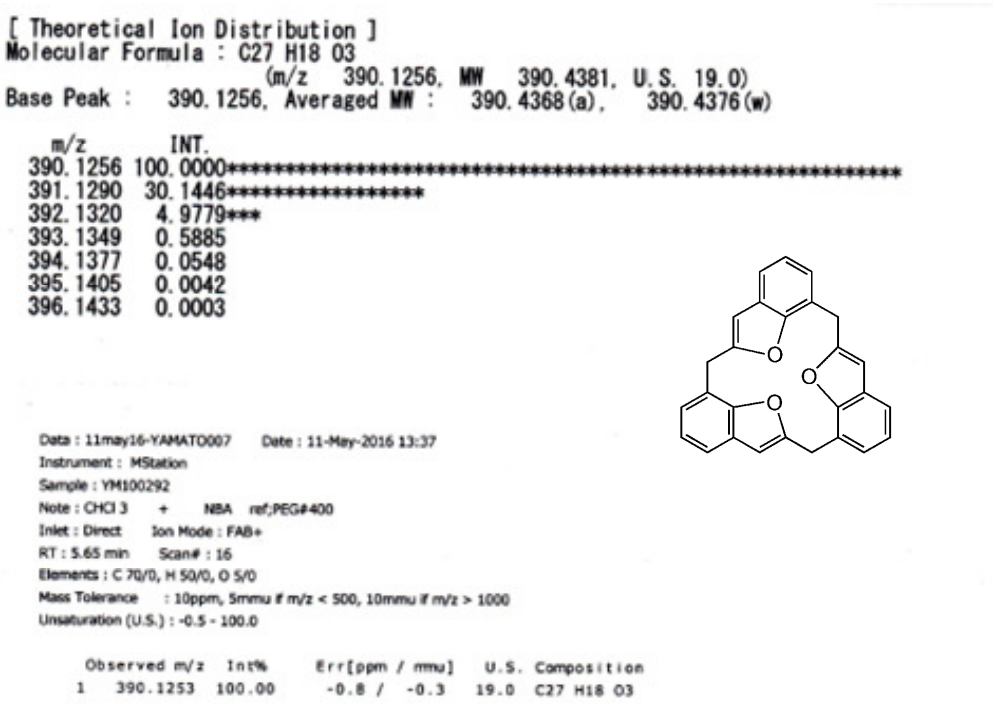

Figure S36: **HRMS** result of the compound **5a**.

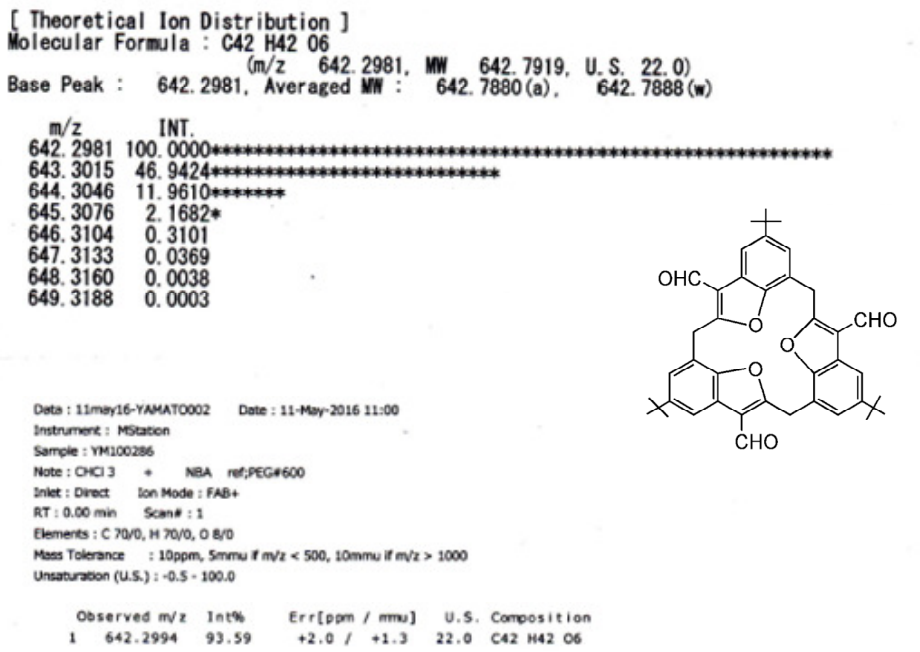

Figure S37: **HRMS** result of the compound **4c**.

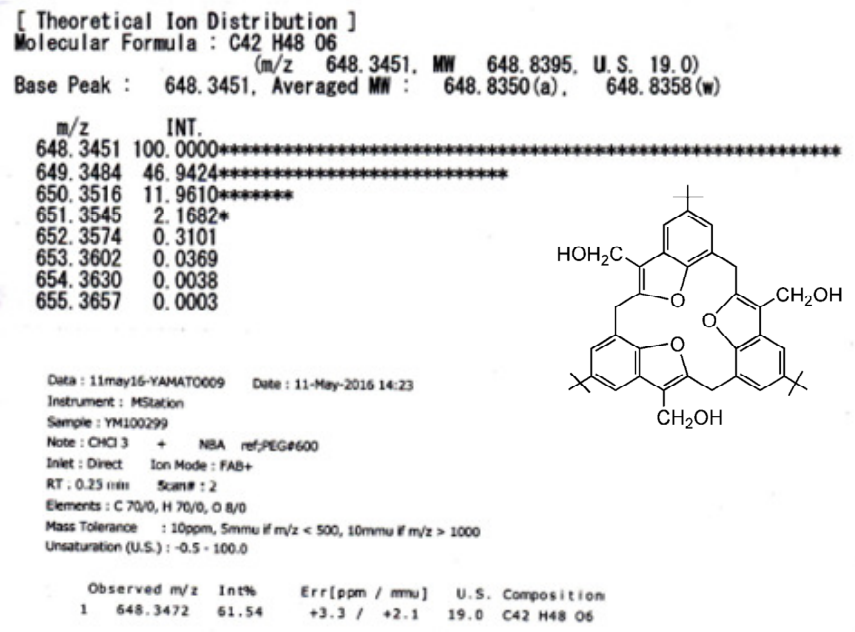

Figure S38: **HRMS** result of the compound **4d**.

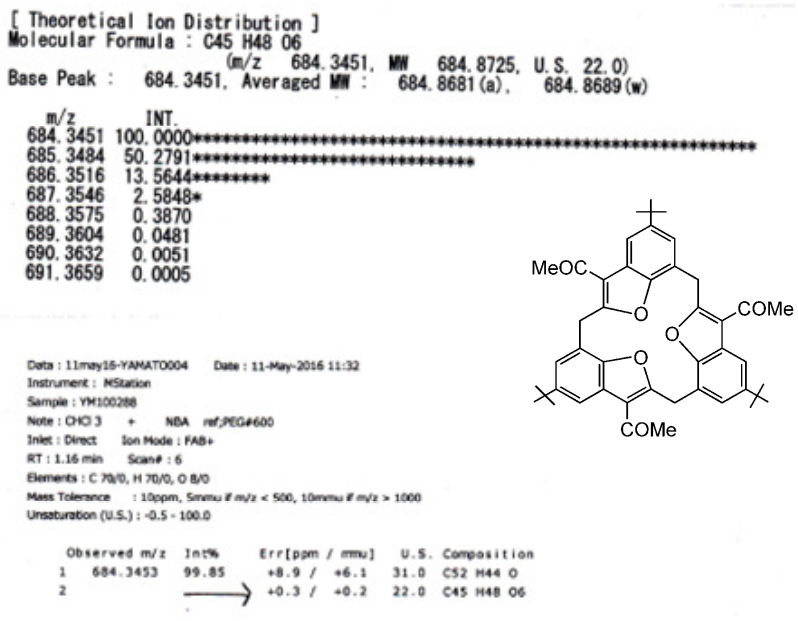

Figure S39: **HRMS** result of the compound **4e**.

X-ray crystallography

Table S1: Summary of crystal data for **4a** and **4b**

Table S1 Summary of crystal data for **4a** and **4b**.[a,b]

Parameter	**4a**	**4b**
Empirical formula	$C_{39}H_{42}O_3$	$C_{39}H_{39}Br_3O_3$, $CHCl_3$, *ca* 6(CH_4O)
Formula weight [g mol^{-1}]	558.76	1107.05
Crystal system	trigonal	trigonal
Space group	*R-3*	*R-3*
A [Å]	19.3942(14)	15.4391(12)
B [Å]	19.3942(14)	15.4391(12)
C [Å]	16.5448(6)	31.782 (4)
α [°]	90.0000	90.0000
β [°]	90.0000	90.0000
γ [°]	120.0000	120.0000
Volume [$Å^3$]	5389.4(6)	6560.8(13)
Z	6	6
Density, calcd [g m^{-3}]	1.033	1.681
Temperature [K]	123	140
Unique reflns	2193	1888
Obsd reflns	1984	1293
Parameters	127	182
R_{int}	0.0399	0.076
R[I>2σ(I)][a]	0.0647	0.072
wR[I>2σ(I)][b]	0.1455	0.138
GOF on F^2	1.154	1.119

[a] Conventional *R* on F_{hkl}: $\Sigma||F_o| - |F_c||/\sigma|F_o|$. [b] Weighted *R* on $|F_{hkl}|^2$: $\Sigma[w(F_o^2 - F_c^2)^2]/\Sigma[w(F_o^2)^2]^{1/2}$

Crystal structure analysis of the tris-benzofuran calixarene, compound 4a:[1–4]

Crystal data: $C_{39}H_{42}O_3$. M = 558.76. Trigonal, space group R-3 (no. 148; hexagonal axes), a = b = 19.3942(14), c = 16.5448(6) Å, α = β = 90, γ = 120 °, V = 5389.4(6) Å^3. Z = 6, Dc = 1.033 g cm^{-3}, F(000) = 3408, T = 123(1) K, μ(Cu-Kα) = 4.96 cm^{-1}, λ(Mo-Kα) = 1.5418 Å.

A colorless prism crystal of $C_{39}H_{42}O_3$ having approximate dimensions of 0.350 x 0.250 x 0.200 mm was mounted on a glass fiber. All intensity measurements were made on a Rigaku R-AXIS RAPID diffractometer using graphite monochromated Cu-Kα radiation. The data were collected at a temperature of -150 ± 1°C to a maximum 2θ value of 136.4°. Of the 20857 reflections collected, 2193 were unique (Rint = 0.0399) and 1984 were 'observed'; equivalent reflections were merged. The linear absorption coefficient, μ, for Cu-Kα radiation is 4.956 cm^{-1}. An empirical absorption correction was applied which resulted in transmission factors ranging from 0.641 to 0.906. The data were corrected for Lorentz and polarization effects. The structure was solved by direct methods[1] and expanded using Fourier techniques. The non-hydrogen atoms were refined anisotropically. Hydrogen atoms were refined using the riding model. The final cycle of full-matrix least-squares refinement on F^2 was based on all 2193 reflections and 127 variable parameters and converged with R_1 = 0.071 and wR_2 = 0.146; for the observed data, R_1 = 0.065. The goodness of fit was 1.15. The maximum and minimum peaks on the final difference Fourier map corresponded to 0.36 and -0.33 eÅ^{-3}, respectively.

Neutral atom scattering factors were taken from International Tables for Crystallography (IT), Vol. C, Table 6.1.1.4.[2] All calculations were performed using the CrystalStructure[3] crystallographic software package except for refinement, which was performed using SHELXL2013.[4]

Crystal structure analysis of a tris-benzofuran calixarene/$CHCl_3$/methanol complex, compound 4b:[5–8]

Crystal data: $C_{39}H_{39}Br_3O_3$, $CHCl_3$, *ca* 6(CH_4O). M = 1107.1. Trigonal, space group R-3 (no. 148; hexagonal axes), a = b = 15.4391(12), c = 31.782(4) Å, α = β = 90, γ = 120 °, V = 6560.8(13) Å^3. Z = 6, Dc = 1.681 g cm^{-3}, F(000) = 3408, T = 140(1) K, μ(Mo-Kα) = 30.1 cm^{-1}, λ(Mo-Kα) = 0.71073 Å.

Crystals are colorless, cubic blocks. One, *ca* 0.43 x 0.37 x 0.25 mm, was mounted in oil on a glass fiber and fixed in the cold nitrogen stream on an Oxford Diffraction Xcalibur-3 CCD diffractometer equipped with Mo-Kα radiation and graphite monochromator. Intensity data were measured by thin-slice ω- and φ-scans. Total no. of reflections recorded, to θ_{max} = 22.5°, was 13024 of which 1888 were unique (Rint = 0.076); 1293 were 'observed' with $I > 2\sigma_I$.

Data were processed using the CrysAlis-CCD and -RED (1) programs. The structure was determined by the direct methods routines in the SHELXS program (2A) and refined by full-matrix least-squares methods, on F^2's, in SHELXL (2B). The analysis shows the calixarene molecule lying around a threefold symmetry axis with, on one side, a $CHCl_3$ solvent molecule (also on the symmetry axis) and, on the other side, a complex ring structure, presumably of a disordered array of methanol molecules; in this region, 50 atoms have been refined as isotropic carbon atoms, mostly with site occupancies of 0.5, about a point of *-3* symmetry. In the calixarene and chloroform molecules, the non-hydrogen atoms were refined with anisotropic thermal parameters; hydrogen atoms were included in idealized positions and their Uiso values were set to ride on the Ueq values of the parent carbon atoms. At the conclusion of the refinement, wR_2 = 0.149 and R_1 = 0.114 (2B) for all 1888 reflections weighted $w = [\sigma^2(F_o^2) + (0.0368P)^2 + 104.34P]^{-1}$ with $P = (F_o^2 + 2F_c^2)/3$; for the 'observed' data only, R_1 = 0.072.

In the final difference map, the highest peak (*ca* 0.37 eÅ^{-3}) was close to Br(13).

Scattering factors for neutral atoms were taken from reference.[7] Computer programs used in this analysis have been noted above, and were run through WinGX (4) on a Dell Optiplex 755 PC at the University of East Anglia.

General description for the DFT computational study:[9,10]

Density functional theory (DFT) computational studies were carried out to determine the geometry-optimized energies of compounds **4a**-**e** and **5a**-**b**. The starting structures were generated with the initial geometries based upon the X-ray structures of **4a** and 4**b** and from the presumed structures of **4c**–**4d** (derived from *cone*-**4a** and *cone*-4**b**) and **5a**–**b** using *SpartanPro'10* with the MMFF94 method.[9] The individual geometry**-**optimized structures of these molecules were first conducted in the gas phase and then in solvent (chloroform) with the B3LYP/6-31G(d) basis set using Gaussian-*09*.[10] The results are summarized in Tables S2 and S3 for both *cone* and *saddle* conformations for compounds **4a**–**e**, **5a**–**b** (Figures S36 to S42). The results presented in Table S2 show that **4a**–**e**, **5a**–**b** were energetically more-favoured in solvent $CHCl_3$ than in the gas phase. The results presented in Table S3 of the synthesized calix[3]benzofurans and their derivatives, **4a**–**e**, suggest that the *saddle* conformers are more stable than the *cone* isomers. The results presented in Tables S2 & S3 show that among the calix[3]benzofurans, **4b** is the energetically most-favoured (in both the solvent and gas-phase) and the order is as follows: **4b>4e>4d>4c >4a>5b >5a** in both the solvent and gas phase. So by introducing the different groups at the furan moieties, the derivatives become energetically more favored over the corresponding calix[3]benzofuran according to the increasing size of groups (i.e. COMe > CH_2OH > CHO) except for **4b**. In the case of **4b**, there may be two factors influencing the stability: bromine is electronegative in nature and has greater electron-density due to multiple lone-pairs of electrons.

The DFT optimized B3LYP/6-31G(d) energies of these two conformers imply that the *saddle* conformers of **4a** and **4b**, which are -4 and -35 $kJmol^{-1}$, are therefore more stable than the *cone* conformers in the solvent, similar to what was computed in gas phase (Table S2). On the other hand, for the *tert*-butyl group analogues, calix[3]benzofuran **5a** and its derivative **5b**, the *saddle* conformers are energetically less stable than the *cone* conformers by 4 and 10 $kJmol^{-1}$ in the gas phase, and by 5 and 7 $kJmol^{-1}$ in solvent (Table S3), respectively. Similarly, *saddle*-**4c**, **4d**, **4e** are energetically more stable by -12, -20 and -48 $kJmol^{-1}$ than *cone*-**4c**, **4d**, **4e** in the gas phase, respectively (Table S3).

Table S2. Geometry optimization energies using B3LYP/6-31G(d)($\Delta E=E_{chlorofom}-E_{gas\text{-}phase}$).

	Cone			***Saddle***		
	Gas phase	Chloroform	ΔE	Gas phase	Chloroform	ΔE
Compound	kJ mol^{-1}	kJ mol^{-1}	kJ mol^{-1}	kJ mol^{-1}	kJ mol^{-1}	kJ mol^{-1}
4a	-4560873	-4560891	-17	-4560878	-4560895	-17
5a	-3322273	-3322291	-18	-3322269	-3322286	-17
4b	-24812139	-24812152	-13	-24812173	-24812188	-15
4c	-5453483	-5453506	-23	-5453495	-5453524	-28
4d	-5462889	-5462924	-35	-5462910	-5462940	-31
4e	-5763178	-5763204	-26	-5763226	-5763254	-28
5b	-4524625	-4524650	-25	-4524615	-4524643	-28

Table S3. Geometry optimization energies using B3LYP/6-31G(d)($\Delta E=E_{Saddle}-E_{Cone}$).

Compound	**Gas-phase**			**Chloroform**		
	Cone	*Saddle*	ΔE	*Cone*	*Saddle*	ΔE
	kJ mol^{-1}	kJ mol^{-1}	kJ mol^{-1}	kJ mol^{-1}	kJ mol^{-1}	kJ mol^{-1}
4a	-4560873	-4560878	-4	-4560891	-4560895	-4
5a	-3322273	-3322269	4	-3322291	-3322286	5
4b	-24812139	-24812173	-34	-24812152	-24812188	-35
4c	-5453483	-5453495	-12	-5453506	-5453524	-18
4d	-5462889	-5462910	-20	-5462924	-5462940	-16
4e	-5763178	-5763226	-48	-5763204	-5763254	-50
5b	-4524625	-4524615	10	-4524650	-4524643	7

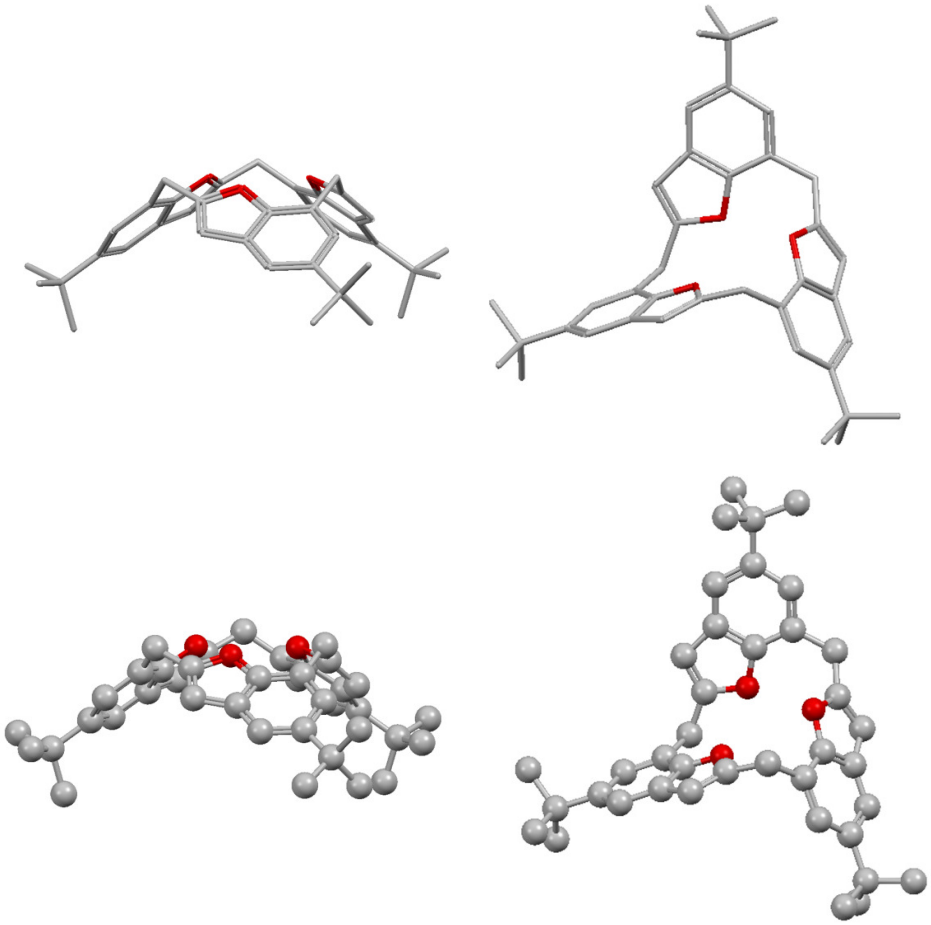

Figure S40. Geometry-optimized (in $CHCl_3$) structures of: *Top Left*: **4a** *cone* (Ellipsoid); *Top Right*: **4a** *saddle* (Ellipsoid). *Bottom Left*: **4a** *cone* (ball-and-stick) and *Bottom Right*: **4a** *saddle* (ball-and-stick). Colour code: carbon = dark grey and oxygen atom = red. All hydrogens are omitted for clarity.

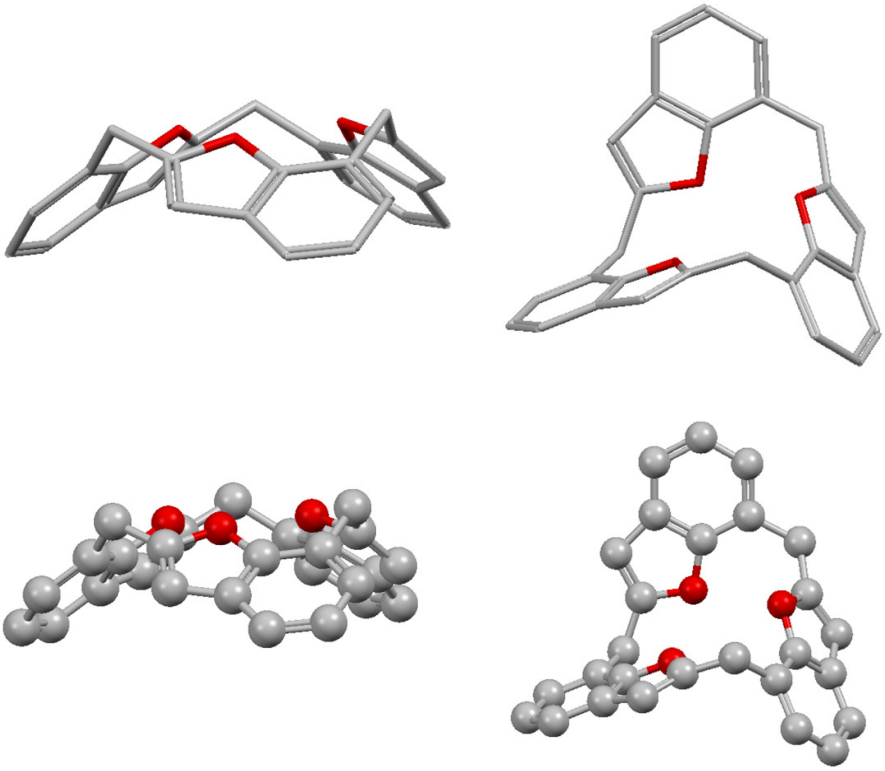

Figure S41. Geometry-optimized (in $CHCl_3$) structures of: *Top Left*: **5a** *cone* (Ellipsoid); *Top Right*: **5a** *saddle* (Ellipsoid). *Bottom Left*: **5a** *cone* (ball-and-stick) and *Bottom Right*: **5a** *cone* (ball-and-stick). Colour code: carbon = dark grey and oxygen atom = red. All hydrogens are omitted for clarity.

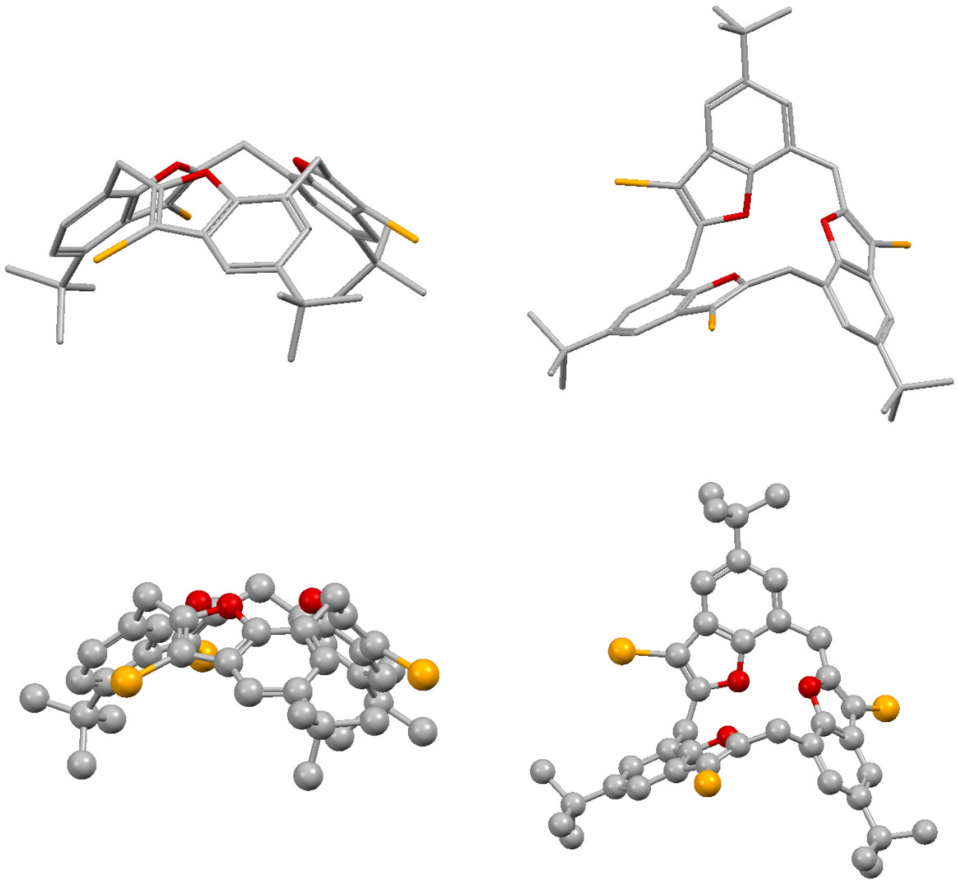

Figure S42. Geometry-optimized (in $CHCl_3$) structures of: *Top Left*: **4b** *cone* (Ellipsoid); *Top Right*: **4b** *saddle* (Ellipsoid). *Bottom Left*: **4b** *cone* (ball-and-stick); and *Bottom Right*: 4b *saddle* (ball-and-stick). Colour code: bromide = orange, carbon = dark grey and oxygen atom = red. All hydrogens are omitted for clarity.

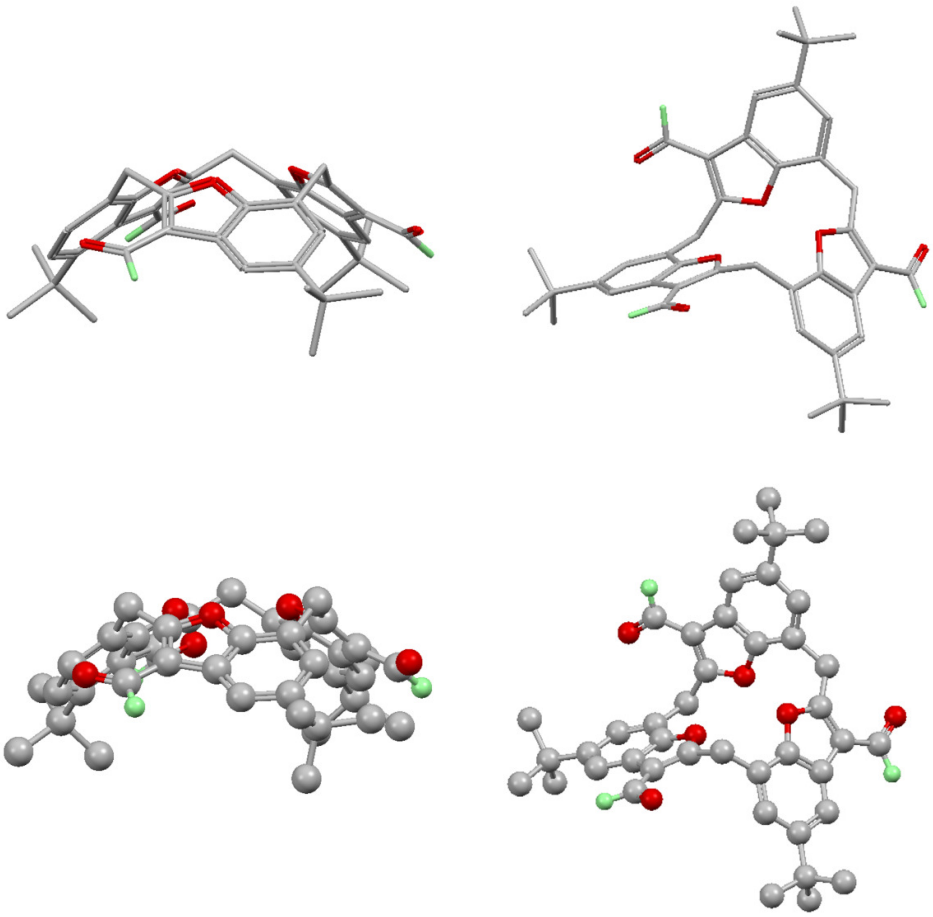

Figure S43. Geometry-optimized (in $CHCl_3$) structures of: *Top Left*: **4c** *cone* (Ellipsoid); *Top Right*: **4c** *saddle* (Ellipsoid). *Bottom Left*:**4c***cone* (ball-and-stick); and *Bottom Right*: **4c** *saddle* (ball-and-stick).Colour code: carbon = dark grey and oxygen atom = red. All hydrogens except aldehyde hydrogen (light green) are omitted for clarity.

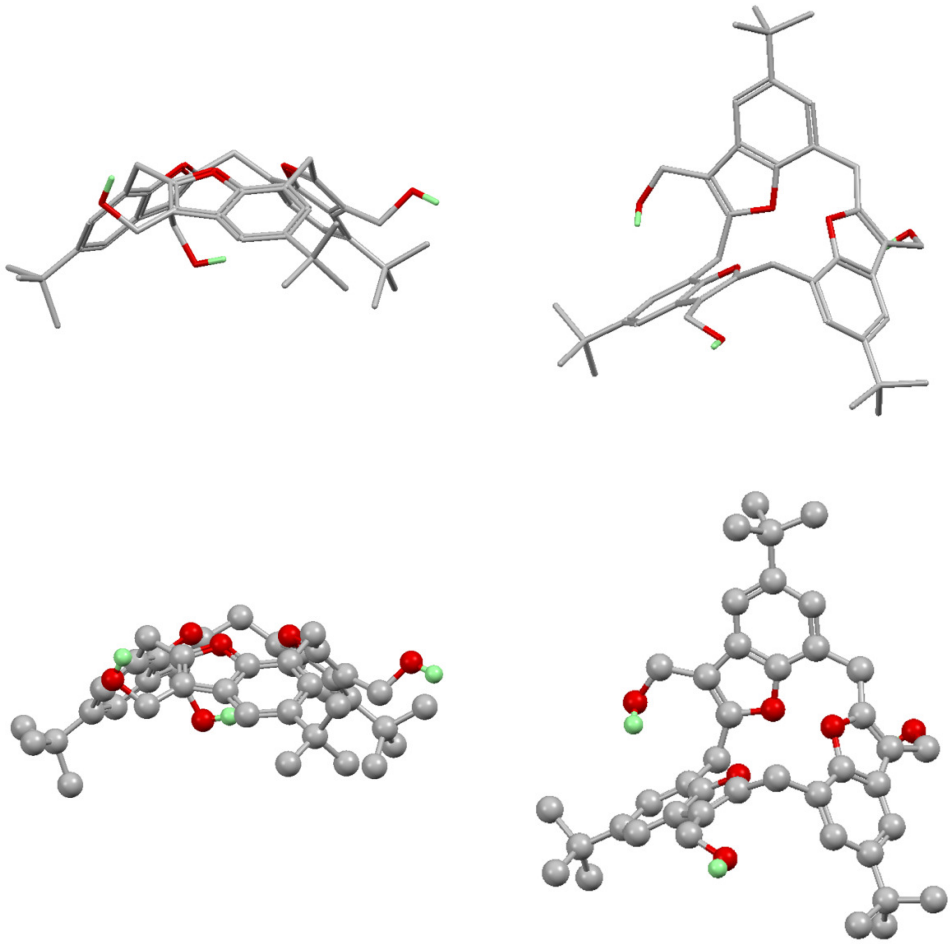

Figure S44. Geometry-optimized (in $CHCl_3$) structures of: *Top Left*: **4d** *cone* (Ellipsoid); *Top Right*: **4d** *saddle* (Ellipsoid). *Bottom Left*:**4d** *cone* (ball-and-stick); and *Bottom Right*: **5c** *saddle* (ball-and-stick).Colour code: carbon = dark grey and oxygen atom = red. All hydrogens except hydroxyl hydrogen (light green) are omitted for clarity.

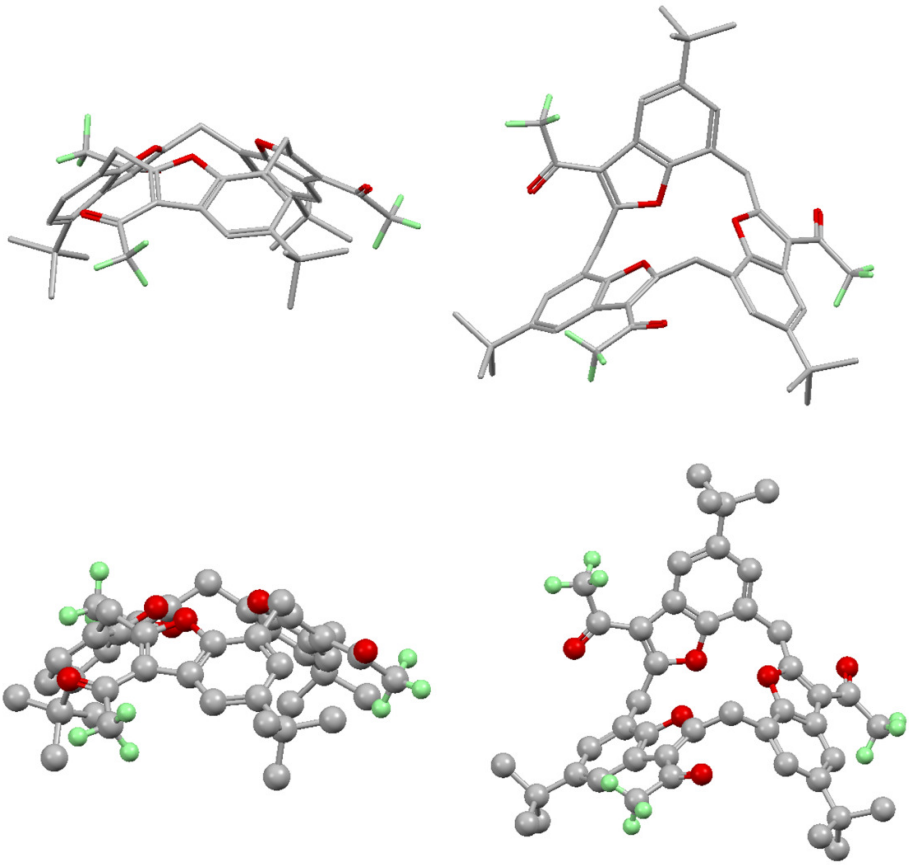

Figure S45. Geometry-optimized (in $CHCl_3$) structures of: *Top Left*: **4e** *cone* (Ellipsoid); *Top Right*: **4e** *saddle* (Ellipsoid). *Bottom Left*: **4e** *cone* (ball-and-stick); and *Bottom Right*: **4e** *saddle* (ball-and-stick).Colour code: carbon = dark grey and oxygen atom = red. All hydrogens except carbonyl hydrogen (light green) are omitted for clarity.

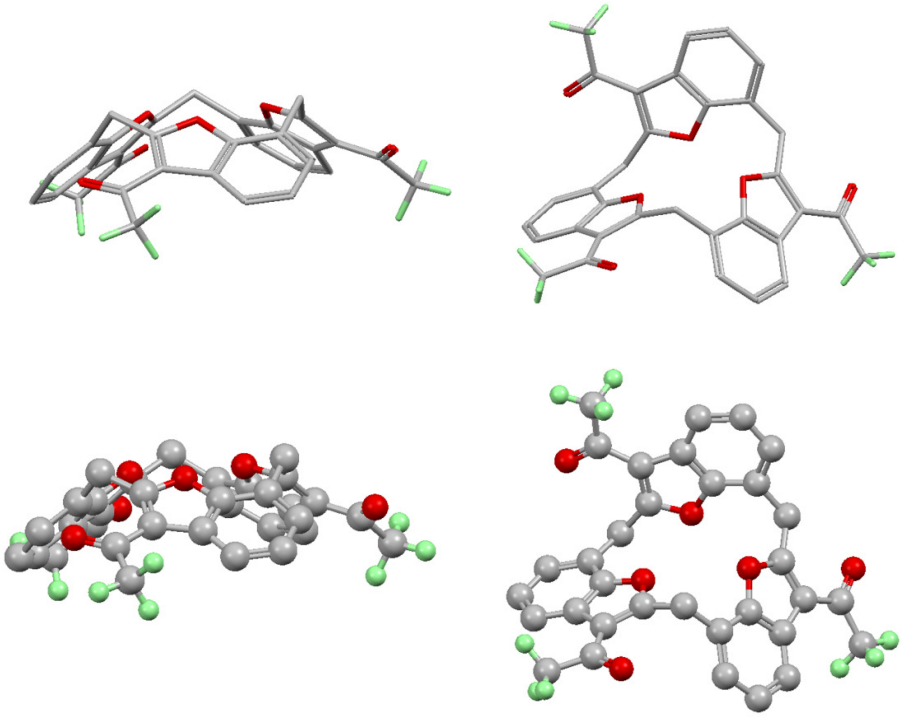

Figure S46. Geometry-optimized (in $CHCl_3$) structures of: *Top Left*: **5b***cone* (Ellipsoid); *Top Right*: **5b** *saddle* (Ellipsoid). *Bottom Left*: **5b** *cone* (ball-and-stick); and *Bottom Right*: **5b** *saddle* (ball-and-stick).Colour code: carbon = dark grey and oxygen atom = red. All hydrogens except aldehyde hydrogen (light green) are omitted for clarity.

References

1. SIR2008: Burla, M. C., Caliandro, R., Camalli, M., Carrozzini, B., Cascarano, G. L., De Caro, L., Giacovazzo, C., Polidori, G. Siliqi, D. and Spagna R. (2007). *J. Appl. Cryst.***40**, 609–613.
2. *'International Tables for Crystallography'*, Vol. C (1992). Ed. A.J.C. Wilson, Kluwer Academic Publishers, Dordrecht, Netherlands, Table 6.1.1.4, pp. 572.
3. CrystalStructure 4.1: Crystal Structure Analysis Package, Rigaku Corporation (2000–2014). Tokyo 196–8666, Japan.
4. SHELXL2013: Sheldrick, G. M. (2008). *Acta Cryst.* A**64**, 112–122.
5. Programs CrysAlis-CCD and -RED, Oxford Diffraction Ltd., Abingdon, UK (2005).
6. G. M. Sheldrick, SHELX-Programs for crystal structure determination (SHELXS-2013) and refinement (SHELXL-2014), *ActaCryst.* (2008) A**64**, 112–122 and (2015) C**71**, 3–8.
7. *'International Tables for X-ray Crystallography'*, Kluwer Academic Publishers, Dordrecht (1992). Vol. C, pp. 500, 219 and 193.
8. L. J. Farrugia, (2012) *J. Appl. Cryst.***45**, 849–854.
9. Initial molecular modeling calculations using the MMFF94 were performed using the PC Spartan'10 software from Wavefunction Inc., Irvine CA.
10. Frisch, M. J.; Trucks, G. W.; Schlegel, H. B.; Scuseria, G. E.; Robb, M. A.; Cheeseman, J. R.; Scalmani, G.; Barone, V.; Mennucci, B.; Petersson, G. A.; Nakatsuji, H.; Caricato, M.; Li, X.; Hratchian, H. P.; Izmaylov, A. F.; Bloino, J.; Zheng, G.; Sonnenberg, J. L.; Hada, M.; Ehara, M.;

Toyota, K.; Fukuda, R.; Hasegawa, J.; Ishida, M.; Nakajima, T.; Honda, Y.; Kitao, O.; Nakai, H.; Vreven, T.; Montgomery, Jr. J. A.; Peralta, J. E.; Ogliaro, F.; Bearpark, M.; Heyd, J. J.; Brothers, E.; Kudin, K. N.; Staroverov, V. N.; Keith, T.; Kobayashi, R.; Normand, J.; Raghavachari, K.: Rendell, A.; Burant, J. C.; Iyengar, S. S.; Tomasi, J.; Cossi, M.; Rega, N.; Millam, J. M.; Klene, M.; Knox, J. E.; Cross, J. B.; Bakken, V.; Adamo, C.; Jaramillo, J.; Gomperts, R.; Stratmann, R. E.; Yazyev, O.; Austin, A. J.; Cammi, R.; Pomelli, C.; Ochterski, J. W.; Martin, R. L.; Morokuma, K.; Zakrzewski, V. G.; Voth, G. A.; Salvador, P.; Dannenberg, J. J.; Dapprich, S.; Daniels, A. D.; Farkas, O.; Foresman, J. B.; Ortiz, J. V.; Cioslowski, J.; Fox, D. J. *Gaussian 09, Revision D.01*; Gaussian, Inc., Wallingford CT, 2013.